UCRL 3240

UNIVERSITY OF CALIFORNIA

Radiation Laboratory

CHEMISTRY DIVISION QUARTERLY REPORT

September, October, November 1955

TWO-WEEK LOAN COPY

This is a Library Circulating Copy which may be borrowed for two weeks. For a personal retention copy, call Tech. Info. Division, Ext. 5545

DISCLAIMER

This document was prepared as an account of work sponsored by the United States Government. While this document is believed to contain correct information, neither the United States Government nor any agency thereof, nor the Regents of the University of California, nor any of their employees, makes any warranty, express or implied, or assumes any legal responsibility for the accuracy, completeness, or usefulness of any information, apparatus, product, or process disclosed, or represents that its use would not infringe privately owned rights. Reference herein to any specific commercial product, process, or service by its trade name, trademark, manufacturer, or otherwise, does not necessarily constitute or imply its endorsement, recommendation, or favoring by the United States Government or any agency thereof, or the Regents of the University of California. The views and opinions of authors expressed herein do not necessarily state or reflect those of the United States Government or any agency thereof or the Regents of the University of California.

UCRL-3240
Chemistry distribution

UNIVERSITY OF CALIFORNIA

Radiation Laboratory
Berkeley, California

Contract No. W-7405-eng-48

CHEMISTRY DIVISION QUARTERLY REPORT

September, October, November 1955

December 20, 1955

Printed for the U. S. Atomic Energy Commission

CHEMISTRY DIVISION QUARTERLY REPORT

September, October, November 1955

Contents

BIO-ORGANIC CHEMISTRY

The Mechanism of the Initial Steps of Reactions in Photosynthesis . . 4

A Study of an Unknown Compound Formed During Photosynthesis in Blue-Green Algae 11

Iron-Chlorophyll Compounds in Green Plants 12

Intermediates in Algae Metabolism 15

Radiation Decomposition of Chlorophyll and Hemin 20

Effects of Ionizing Radiation on Choline Analogs 21

Preparation of Calcium Glycolate for Radiation Sensitivity Studies 22

Partition Chromatography of Carbon Dioxide 23

The Resolution of DL-Valine 24

Synthesis of Glycine-2-C^{14} via an Improved Methanol-C^{14} Preparation 25

Preparation of DL-Carnitine Hydrochloride 27

Liquid Scintillation Counting of Tritium by Means of Coincidence Techniques. 28

Lipogenesis in the Adipose Tissue of the Intact Rat 35

Respiratory Metabolism of Acetate, Glucose, and Glycine in the Hereditary Obesity-Diabetes Syndrome of Mice . . 36

$C^{14}O_2$ Excretion Patterns and Metabolic Activity Level in Rats 46

The Incorporation of Adenine-2-C^{14}, Adenine-8-C^{14}, and Adenine-4, 6-C^{14} into Nucleotides and Nucleic Acids in C_{57} Mice 55

NUCLEAR CHEMISTRY

Optical Spectroscopy

Color Centers and Luminescence in Lanthanum Chloride-Europium Chloride Crystals 62

Low-Temperature Dewar for Zeeman Effect in Absorption 62

Three-Millisecond Metastable State in Lead-209 63

---

* Preceding Quarterly Reports: UCRL-3157, UCRL-3068.

The Crystal Structure of Americium Metal 63
The Reaction Products of Tantalum with 5.7-Bev Protons . . 64
Ion-Exchange Equilibrium Studies 65
Electron-Capture Decay of Polonium-206 65
Fission-Spallation Mechanisms
Fission and Spallation Reactions of Americium-241 with Low-Energy Alpha Particles 66
Fission and Spallation Reactions of Uranium-235 with Low-Energy Alpha Particles 68
Fission and Spallation Reactions of Protactinium-231 with Low-Energy Alpha Particles 69
Tritium Production in Heavy-Element Cyclotron Targets 69
Radiation Chemistry 70
Alpha-Particle Spectroscopy 72
Electron Spectroscopy 74
The Interaction of High-Energy Protons with Nuclei: an Interpretation of Radiochemical Results 75

CHEMICAL ENGINEERING (PROCESS CHEMISTRY)
Notes on Work in Progress 80

GENERAL CHEMISTRY
Metals and High-Temperature Thermodynamics 82
Basic Chemistry
Ruthenium Chemistry 83
Kinetics of Rapid Reactions 84
Polarographic Studies 84
Radiation-Induced Reactions in Nonaqueous Solutions . . 84
Determination of the Molecular Structure of Aluminum Hydride 85
Mechanism of Electroreduction 85
Heat of Formation of the Ferrate Ion 85
Acetaldehyde, t 85

CHEMISTRY DIVISION QUARTERLY REPORT

September, October, November 1955

Radiation Laboratory; Department of Chemistry; and
Donner Laboratory of Biophysics and Medical Physics
University of California, Berkeley, California

December 20, 1955

BIO-ORGANIC CHEMISTRY

M. Calvin, Director
Edited by B. M. Tolbert

THE MECHANISM OF THE INITIAL STEPS OF REACTIONS IN PHOTOSYNTHESIS

J. A. Bassham and Kazuo Shibata

Many experiments have been carried out with intermittent light to see the mechanism of the initial steps of reactions in photosynthesis. But, as was pointed out in the previous report, most attention has been paid to the change of the photosynthetic yield per flash in a fixed period, with different dark periods. From the results, different theories were proposed. According to the experiment by R. Emerson and W. Arnold,[1] the theory of a "photosynthetic unit"[2, 3] was proposed. By the more precise study by Tamiya and Chiba,[4] it was found that the maximum yield becomes temperature-dependent when the light intensity is very high, which contradicts the theory of a "photosynthetic unit." In place of this theory, Tamiya and Chiba proposed a different mechanism in which the sensitizer S (probably chlorophyll or a state of chlorophyll) is converted to the excited sensitizer S*, and S* reacts with the other chemicals for photosynthesis or it is deactivated by the second-order temperature-dependent reaction. In spite of the quite different mechanisms in these theories, there is similarity in one respect; namely, they assumed only one compound to be excited or one reservoir to be filled during the course of a flash, with other steps in photosynthesis following in the dark period. For the sake of convenience, we designated this type of theory as "one-reservoir theory."

---

1 R. Emerson and W. Arnold, J. Gen. Physiol. 15, 391 (1932); 16, 191 (1933).

2 H. Gaffron and K. Wohl, Naturwissenschaften 24, 81, 103 (1936).

3 K. Wohl, Z. Physik. Chem. B, 37, 105, 122, 169, 186, 209 (1937); New Phytologist 39, 33 (1940), 40, 34 (1941).

4 H. Tamiya and Y. Chiba, Studies of the Tokugawa Institute 6, No. 2 (1949).

The experiment reported here was carried out to see the effect of flashing light period on the maximum yield per flash with long dark period and with high intensity that is great enough to saturate photosynthesis even with the flashing light. As will be shown later, it is necessary to assume that at least two reservoirs are filled, or partially filled, in the course of light period in order to explain the results obtained.

Methods

The system used in this experiment is the same as the system for our quantum requirement experiments,[5] although the total volume was changed to increase the sensitivity, and the surface area of the cell for algal suspension was reduced to obtain more light per unit area of the suspension of algae. The photosynthetic rate was measured by observing the change of oxygen content in the closed system by means of an analyzer measuring the paramagnetic property of oxygen. At the same time, the change of CO_2 was observed as a reference by an infrared CO_2 analyzer. To saturate the photosynthetic yield, two 1-kw projection lamps and a 400-w photospot illuminated the suspension of algae through two sheets of infrared absorbing glass with a water cooling system. In front of the cell, which contained 25 ml of algal suspension, a disk with open sectors was rotated. Six kinds of disks were used; they have 1, 2, 3, 4, 6, and 9 open sectors, equal in size, in a disk 40 cm in diameter. The size of opening was chosen so that with a 9-hole disk the dark and light periods are equal. Therefore, the ratios of the dark periods to the light periods in these different disks are 17, 8, 5, 3, 5, 2, and 1, respectively. If the rate of rotation is fixed, the light period (t_e) is the same for each sector, but the dark period (t_d) can be changed by changing the disk. From a set of data with a single rotating rate, one can obtain the change of yield per flash as a function of dark period for a fixed light period. The light period was changed by changing the rotating rate. The light periods were 1/360, 1/180, 1/90, and 1/45 sec.

The important point in this experiment is that the photosynthetic rate should be saturated with respect to light intensity under the conditions used. The saturation was tested with the longest dark periods (one-hole disk) for two light periods, 1/360 sec and 1/45 sec. One of the results with $t_e = 1/360$ sec and $t_d = 17/360$ sec is shown in Fig. 1, where relative photosynthetic rate per flash (P_f) is plotted against the relative light intensity (I_{rel}). The arrow in the figure indicates the working condition of light intensity with which the further flashing-light experiments were carried out. With this light intensity, the yield is well saturated even with the one-hole sector. The concentration of the suspension of Scenedesmus was 0.2% in packed cell volume units.

Results

The results are shown in Fig. 2, where the relative photosynthetic rate per flash (P_f) was plotted against dark period (t_d). Each curve represents the change of photosynthetic rate for a particular light period (t_e) as a function of dark period. The points for zero dark period were calculated from the continuous light rate. The relative unit of P_f was

---

[5] J. A. Bassham, K. Shibata, and M. Calvin, Biochim. Biophys. Acta 17, 332 (1955).

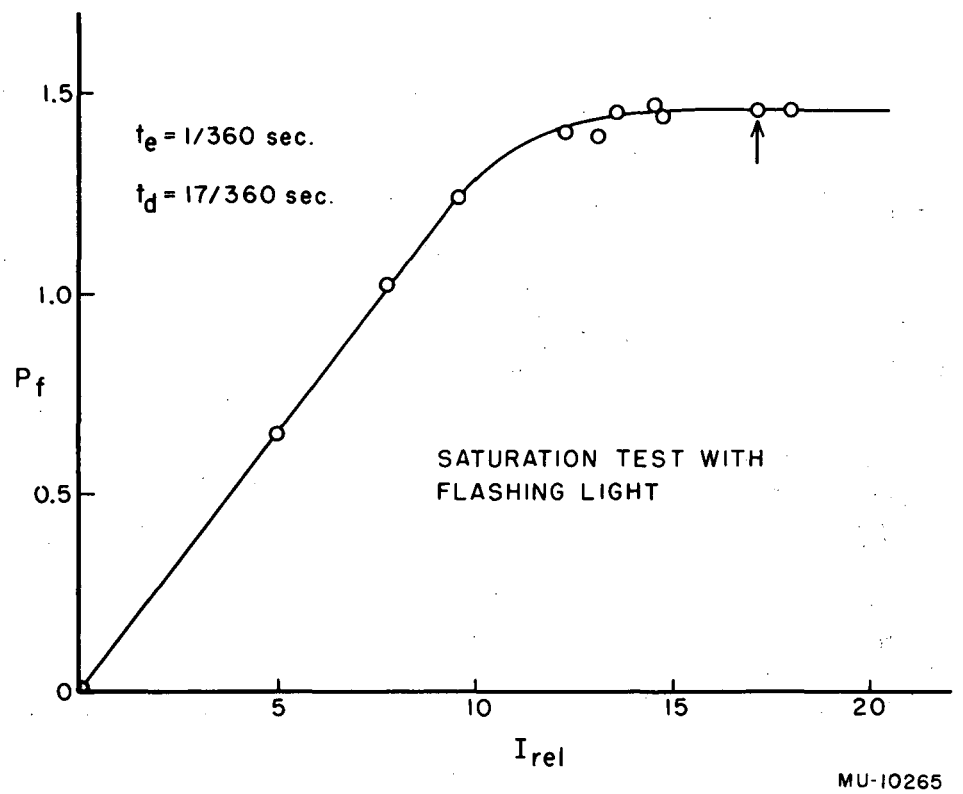

Fig. 1. Saturation test with flashing light.

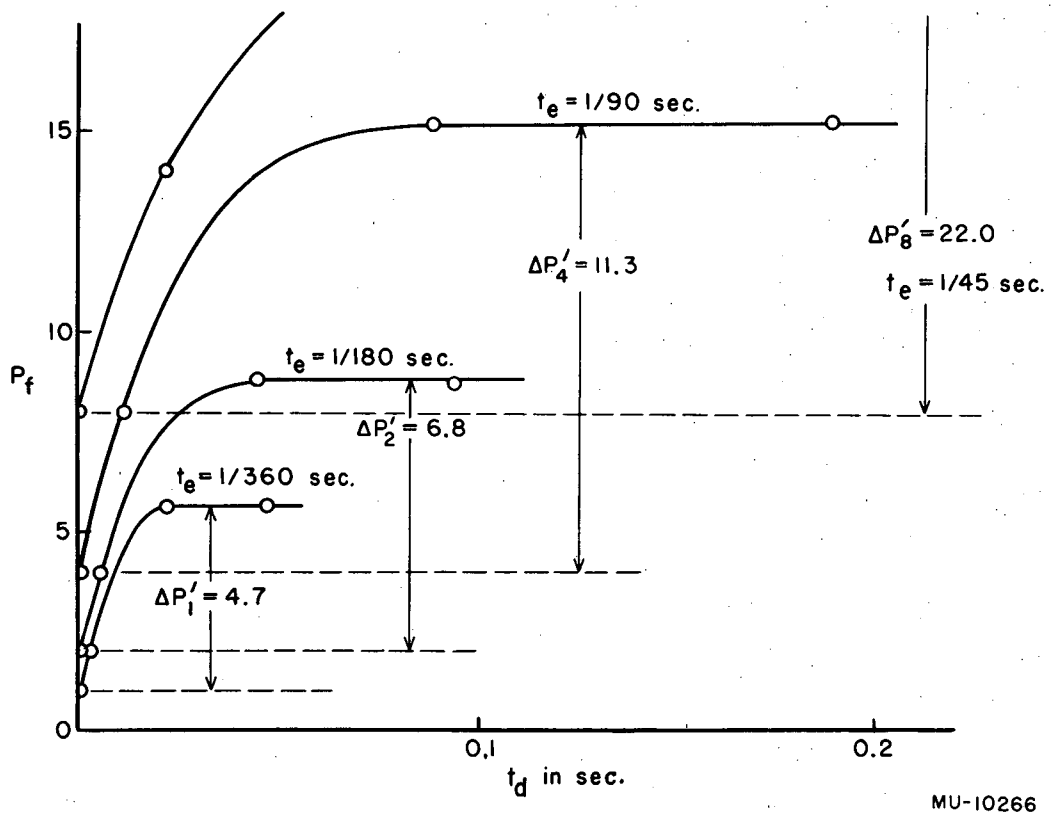

Fig. 2. Change of oxygen generation per flash with changing dark periods.

chosen so as to make P_f for t_e = 1/360 sec and t_d = 0 sec equal to unity so that the value for the intercepts for the curves at t_e = 1/360, 1/180, 1/90, and 1/45 sec are 1, 2, 4, and 8, respectively. As will be seen in this figure, P_f goes up linearly at the beginning and levels off to a maximum value. The behavior of this change of P_f with dark period agrees with the results that have been obtained by other investigators.

For the purpose of discussion the effect of the variation in light period, $\Delta P'_e$, was defined as the difference between the P_f value for zero dark period and the maximum P_f value for each curve. The subscript e indicates the relative light period and prime means that it is a relative value. Table I gives $\Delta P'_e$ and the corresponding absolute value ΔP_e.

Table I

Extra yield of oxygen per flash in photosynthesis as a function of flash time

Ch (total Chlorophyll-a content) = 117×10^{-8} mole/25 ml of suspension

t_e	$\Delta P_i'$	ΔP_i (10^{-8} mole/25 ml)	ΔP_i/Ch (%)
1/360	4.69	3.80	0.325
1/180	6.75	5.62	0.480
1/90	11.28	9.12	0.782
1/45	22.00	17.8	1.517
0	3	2.43	0.204

The quantity $\Delta P'_e$ is the measure of the additional oxygen generation per flash in the dark above the oxygen generation in the light; $\Delta P'_e$ is changed by the intermediates stored in the light. First, let us consider the effect of light period on $\Delta P'_e$ based on the "one-reservoir theory." In the course of the light period, the reservoir is filled by the energy of light, and should be full by the end of the light period because the photosynthetic rate is saturated against light intensity. Presumably, the initial step of this process would be photochemical reaction, and some purely chemical reaction may follow it, or some deactivation may be included in a complicated way. But, as long as we assume only one reservoir that is responsible for the further reactions of photosynthesis, $\Delta P'_e$ should be constant and independent of light period, because the light intensity is strong enough to saturate the reservoir in any light period used. This must be true, no matter what the mechanism of reactions relating to this particular reservoir may be.

In Fig. 3 $\Delta P'_e$ is plotted against relative light period. As will be seen in this figure, $\Delta P'_e$ increases with increasing light period instead of staying constant at the level indicated by the dotted horizontal line in the figure. The curve becomes an almost straight line at longer light periods.

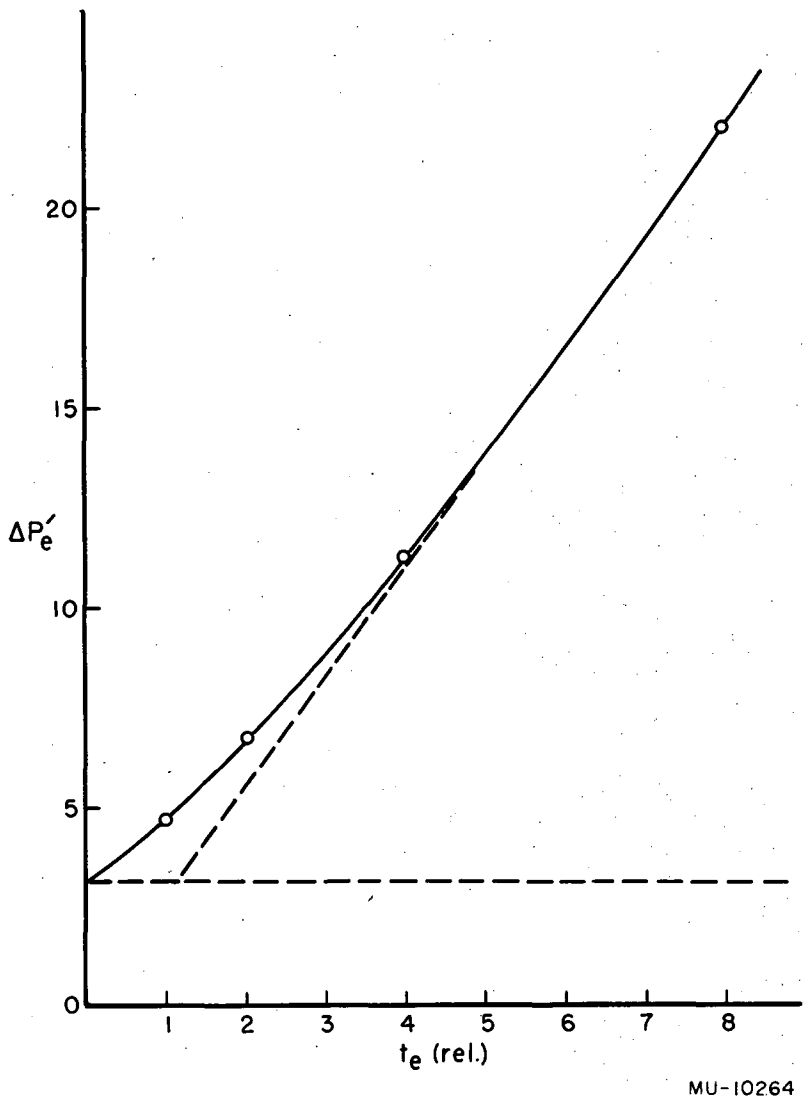

Fig. 3. Oxygen generation per flash as a function of light period.

This result indicates that we must assume two reservoirs even in these short light periods to explain the effect of varying light periods on ΔP_e. The size of the first reservoir is about 3 in terms of $\Delta P'_e$ and almost from the beginning the second reservoir begins to be filled, as can be seen from the fact that the straight part of the curve can be extrapolated to pass through the origin. The ratio of ΔP_e (absolute value) to total chlorophyll amount of the sample of algae was also listed in Table I. The ratio extrapolated to zero light period is 0.204%, the reciprocal of which is about 481 molecules. This number is much smaller than the photosynthetic unit of 2500, which might be caused by weak light intensity.

Another fact we might point out is that the first reservoir is almost filled at about 3 milliseconds. This time is calculated from the intersection of the horizontal straight line and the extrapolated line from the straight part of the curve in Fig. 3. This time corresponds to the first fast decay period of chemiluminescence, which was observed by Strehler et al.[6]

The straightness of the curve in Fig. 3 at longer light periods indicates that the second reservoir is filled by a zero-order reaction, which is quite reasonable as an enzymatic reaction. If the light period is further increased, the curve in Fig. 3 may level off when the second reservoir is saturated. The systematic study of the $\Delta P'_e$ curve with the effect of various chemical inhibitors provides further information on the mechanism of reactions of the early steps following the photochemical reactions in photosynthesis.

---

[6] B. Strehler, Arch. Biochem. Biophys. 34, 239 (1951);
B. Strehler and W. Arnold, J. Gen. Physiol. 34, 809 (1951);
W. Arnold and J. B. Davidson, J. Gen. Physiol. 37, 677 (1954);
B. Strehler, reported at Gatlinburg Meeting on Photosynthesis, 1955;
W. Arnold, reported at Gatlinburg Meeting on Photosynthesis, 1955.

A STUDY OF AN UNKNOWN COMPOUND FORMED DURING PHOTOSYNTHESIS IN BLUE-GREEN ALGAE

P. Linko and O. Holm-Hansen

During the past three months, efforts have been made to elucidate the nature of the unknown compound that has been reported to occur in blue-green algae under short-time photosynthesis experiments. As Norris, et al.[1] have reported that this unknown substance accounts for as much as 21% of the total radioactive carbon incorporated during 5 minutes of photosynthesis by the alga Nostoc muscorum, it is of great interest to identify this substance and elucidate its role in these algae.

As the published report by Norris did not indicate the degree of reproducibility of the occurrence of this unknown compound, and as the work on this subject by M. Thain was inconclusive, an attempt was made to reproduce the work of Norris. Many difficulties have arisen in the attempt to follow Norris's procedure, and after three months of altering both the growth conditions and for the algae the experimental conditions, the unknown spot on the radioautograms has been found, but in concentrations far less than that reported by Norris. One difficulty that should be mentioned is that cells of Nostoc muscorum burst when transferred from the normal nutrient solution to distilled water. The Nostoc muscorum used now has recently been obtained from Dr. M. B. Allen, and hence the question arises as to the particular Nostoc strain that Norris employed.

Another difficulty has been the presence of two unknown spots on the radioautogram, instead of just one. In old chromatograms left in the laboratory by Norris (?), it appears that there may be a confusion between these two spots, as chromatograms have been found where the unknown spot reported in Norris's paper is very light (call this spot A), while the second unknown spot (spot B) has been quite heavy. Scenedesmus has also been tested, and spot B has been found, but in very low concentration compared to that in Synechococcus and Nostoc. From the location of spot B on the chromatogram, it was suspected that it was glutamine. To test this, spot B was eluted, hydrolyzed in 1 N HCl for one hour in a sealed tube at 105° C, and rechromatographed, both with and without labeled glutamic acid. It appears that this treatment hydrolyzed the unknown compound B and formed only one new active compound. The location of this new spot was exactly that of glutamic acid, so it has been assumed that this spot B is actually glutamine. The hydrolysis treatment as above did not, however, affect spot A, in direct contrast to what was reported in Norris' paper. This unknown has been shown in our experiments to be weakly ninhydrin-positive, and to remain quantitatively with the amino acid fraction when the total ethanol extract is put through a Dowex 50 column. Experiments at the present time are concerned with trying to procure information concerning the chemical nature of this unknown substance by using hydrolysis (varying conditions), hydrogenation, deamination, and various color reactions for specific chemical groups. In addition, of course, attention is still being directed to the general experimental conditions, in an attempt to clarify the discrepancies noted between this work and that of Norris.

---

[1] Louisa Norris, R. E. Norris, and M. Calvin, University of California Radiation Laboratory Report No. UCRL-2565, May 1954.

IRON-CHLOROPHYLL COMPOUNDS IN GREEN PLANTS

Jean Bourdon

The conversion of the energy of light to the energy of chemical compounds required by the photosynthetic cycle in green plants is believed to be accomplished by the pigment system, which transforms electromagnetic energy to electronic potential energy.[1] In this theory, chlorophyll molecules absorb light quanta and are raised energetically to an excited electronic state which can be transferred from one chlorophyll molecule to another (exciton migration). A special pigment is then required which upon being excited, could convert the energy of its excited state to a separation of charges by the emission of an electron. This might be achieved by a molecule of chlorophyll containing some metal other than magnesium, where the metal has two levels of oxidation, for instance iron, manganese, or copper:

$$h\nu + Chl_{Mg^{++}} \rightarrow Chl^{*}_{Mg^{++}} ,$$

$$Chl^{*}_{Mg^{++}} + Chl_{Fe^{++}} \rightarrow Chl_{Mg^{++}} + Chl^{*}_{Fe^{++}} ,$$

$$Chl^{*}_{Fe^{++}} \rightarrow Chl_{Fe^{+++}} + e^{-} .$$

The electron would then be transferred by semiconductors to an electron acceptor while the $Chl_{Fe^{+++}}$ would remove an electron from water and be reduced to $Chl_{Fe^{++}}$. This metal-chlorophyll compound might be present only in very slight amounts (perhaps 1/1000 of the content of chlorophyll), inasmuch as it need act only as a converter of energy.

It will be remembered that many pigments containing iron exist in green plants in the form of cytochromes, but these are usually considered to be functioning in respiration processes and perhaps in photosynthetic phosphorylation. Cytochrome-f and b_6 are found only in chloroplasts and might be related to photosynthesis.[2] These pigments are closely related to heme rather than to chlorophyll.

However, Askinazi and co-workers[3] have found that when an alcoholic solution of chlorophyll is treated by an iron salt ($FeCl_3$) an exchange between magnesium and iron takes place and the chlorophyll is then found to contain only iron. In another paper, Askinazi[4] showed that these iron chlorophyll compounds are reduced by light under nitrogen and oxidized by air, this oxido-reduction being reversible.

---

1 J. A. Bassham and M. Calvin, University of California Radiation Laboratory Report No. UCRL-2853, February 1955.

2 R. Hill and R. Scarisbrick, New Phytologist 50, 98 (1951); H. E. Davenport, Nature 170, 1112 (1952); R. Hill, Nature 174, 501 (1954).

3 M. S. Askinazi, T. S. Glickman and B. Dahn, Dokl. Acad. Nauk. SSSR 73, 743 (1950).

4 M. S. Askinazi and V. E. Kartpitskaya, Dokl. Acad. Nauk. SSSR 96, 785 (1954).

Considering the large content of iron in chloroplasts and the ease with which the formation of iron chlorophyll is accomplished, it is natural to assume that those complexes can also be formed in chloroplasts. Consequently, an investigation has been made of this possibility.

Many different extractions and separations of plant pigments have been carried out so far and such an iron chlorophyll has not yet been found. This may be because of the very small amounts of such a compound. The investigation is now being continued with the use of radioactive iron, Fe^{59}, and we hope by this very sensitive means to be able to find evidence of this hypothetical compound.

Methods to be used

(a) Extraction of pigments of green plants grown in a medium containing a salt of radioactive iron, followed by separation of the various pigments and a check of the radioactivity in the different fractions.

(b) Introduction of a sample of synthetic radioactive iron chlorophyll in the crude extract and a check to see if the radioactivity is identical in its location to any of the fractions in (a), indicating the possible presence of iron chlorophyll.

(c) Identification of iron chlorophyll by ultraviolet spectra.

Experimental

The radioactive iron used was Fe^{59} (half life = 47 days) as ferrous citrate or ferric chloride. The plants studied were algae (Chlorella, Scenedesmus) and beans. Extraction of plants was done by alcohol, cold or hot, or by cold acetone. Preparation of iron chlorophyll (hematin pheophytin)[5] was done in two ways:

(a) Pure chlorophyll a was prepared from spinach by extraction with acetone, then purified by two chromatographies on sugar according to Winsterstein and Stein.[6] The chlorophyll a treated by HCl in EtOH gave pure pheophytin a.

(b) Pheophytin a could also be obtained in almost the same state of purity directly from grass, on a larger scale, by action of HCl on the alcoholic extract, then purification by extraction.

Purity of all these compounds was checked by ultraviolet and infrared spectra. Purity of pheophytin was checked by chromatography and ultraviolet spectrum. Iron chlorophyll was obtained from pheophytin a, according to Kunz, Morneweg, and Muller,[5] by action of iron and sodium chloride in an acetic acid solution at 80°. The compound obtained contained

[5] K. Kunz, M. Morneweg and H. Muller, Z. physik. Chem. 199, 93 (1931).

[6] A. Winsterstein and G. Stein, II. Z. physiol. Chem. 220, 263 (1934).

one atom of chlorine; the iron was in the oxidized state. It is a blue-black powder giving a deep green solution. The ultraviolet and infrared spectra are almost identical to those of chlorophyll. Some spectral studies were done on this compound: transformation as a function of pH and oxygen tension.

The radioactive compound was prepared by the same method but with the addition to the reaction solution of 10 μc of ferrous citrate (0.1 cc of solution for 20 mg of pheophytin).

Chromatography of Iron Chlorophyll

We wanted to see if the iron chlorophyll could be separated from ordinary chlorophyll by chromatography. As a matter of fact, some separation takes place when the chromatography is done on a sugar column with a mixture of petroleum ether and benzene as solvent. The separation was not very good and only a small part of the iron compound could be recovered. Then a sample of radioactive iron chlorophyll was introduced into an alcoholic extract (hot extraction) of algae, and after the usual treatment for isolation of chlorophyll, we found that most of the radioactivity was lost. Only 1/4 was found on the column and 1/9 in the higher fraction which showed the spectrum of iron chlorophyll.

Despite this not very encouraging result, we grew Chlorella in a solution containing 40 μc of radioactive iron. The alcoholic extract was made after 24 hours and chromatographed as above. Most of the radioactivity was lost once more and all the fractions were found to contain some radioactivity.

Conclusion

These results might be attributed to either the low solubility of iron chlorophyll in petroleum ether or to the alteration of this compound during the treatment or on the sugar. To overcome the solubility problem one might use an iron compound bound to pyridine instead of chlorine, but this approach to the problem has not been pursued yet. Instead we have undertaken the following approach: (a) make a cold extract instead of a hot one, (b) obtain a cytochrome-free chlorophyll preparation, (c) study the introduction of radioactive iron in the cytochrome fraction and compare with their concentration and oxidation state as indicated by the intensity of their spectra.

Hill,[2] working with bean leaves, could determine the presence of cytochromes in cold acetone powder by their ultraviolet spectrum. If beans are ground in the presence of acetone, one can get a deep-green acetone solution containing pigments and a colorless powder containing the cytochrome.

The spectrum of this powder was measured by making a paste with a solution of sodium hydrosulfite and placing this paste in a 2.5-mm cell (according to Shibata's technique[7]). From this crude paste we were able to get a spectrum of the reduced cytochrome (560 and 530) very similar to the one of pure cytochrome b_3 obtained by Hill. These results were rather quantitatively reproducible (20%).

---

[7] K. Shibata, A. A. Benson, and M. Calvin, UCRL-2635, June 1954.

Recently the beans were grown in a nutrient solution containing a salt of radioactive iron ($FeCl_3$). We are repeating the separation procedure, and at the same time measuring the radioactivity. We have found practically all the radioactivity in the acetone powder and only a very low activity in the crude acetone solution of pigments (about 1.5%). The next step will be the separation of these pigments.

INTERMEDIATES IN ALGAE METABOLISM

James A. Bassham, S. Alan Barker, and V. Carol Quarck

This report deals with the results of (a) a search for tetrose and xylulose phosphates among the photosynthetic products of Scenedesmus and (b) some preliminary studies on several unidentified nucleotides, phosphates, and oligosaccharides.

Paper Ionophoresis

In order to acquire information additional to that obtainable from the normal two-way paper chromatograms in phenol-water and butanol-propionic acid, an improved paper electrophoresis apparatus[1] was assembled. The separation of many sugars, as their borate complexes, could be accomplished after 3 hr at 600 v using borate buffer of pH 10.0 as the electrolyte.[2] The method of Wade and Morgan[3] for the separation of sugar phosphates was modified by the substitution of propionic acid (222 g), sodium hydroxide (3 g), and water (2.76 l) for the odorous n-butyric acid–sodium hydroxide electrolyte. This method will separate sugar monophosphates from sugar diphosphates but in general will not separate isomeric phosphates. Separations of the latter type (e.g. glucose-1-phosphate from glucose-6-phosphate; fructose-6-phosphate from fructose-1-phosphate; glucose-1-phosphate from fructose-6-phosphate) were, however, achieved by using borate buffer of pH 10.0 as the electrolyte. It was found that a ferric chloride-sulfosalicylic acid spray[3] or a modified silver nitrate spray[4] were sometimes superior to the normal perchloric acid–ammonium molybdate spray for detecting sugar phosphates. In particular, the silver nitrate reagent was excellent for detecting reducing sugar phosphates.

Tetrose and Xylulose Phosphates

It has been postulated (M. Calvin and J. A. Bassham, private communication) that in the photosynthetic cycle the action of transketolase on a mixture of fructose-6-phosphate and 3-phosphoglyceraldehyde should yield erythrose-4-phosphate and xylulose-5-phosphate (Fig. 4). The object of our investigation was to attempt to identify the two latter compounds among the products of photosynthesis by Scenedesmus and to determine whether a reserve source of these might be their corresponding diphosphates.

---

[1] A. B. Foster, Chem. and Ind. 1952, 1050.

[2] A. B. Foster, J. Chem. Soc. 1953, 982.

[3] H. E. Wade and D. M. Morgan, Biochem. J. 60, 264 (1955).

[4] W. E. Treveleyan, D. P. Procter and J. S. Harrison, Nature 166, 444 (1950).

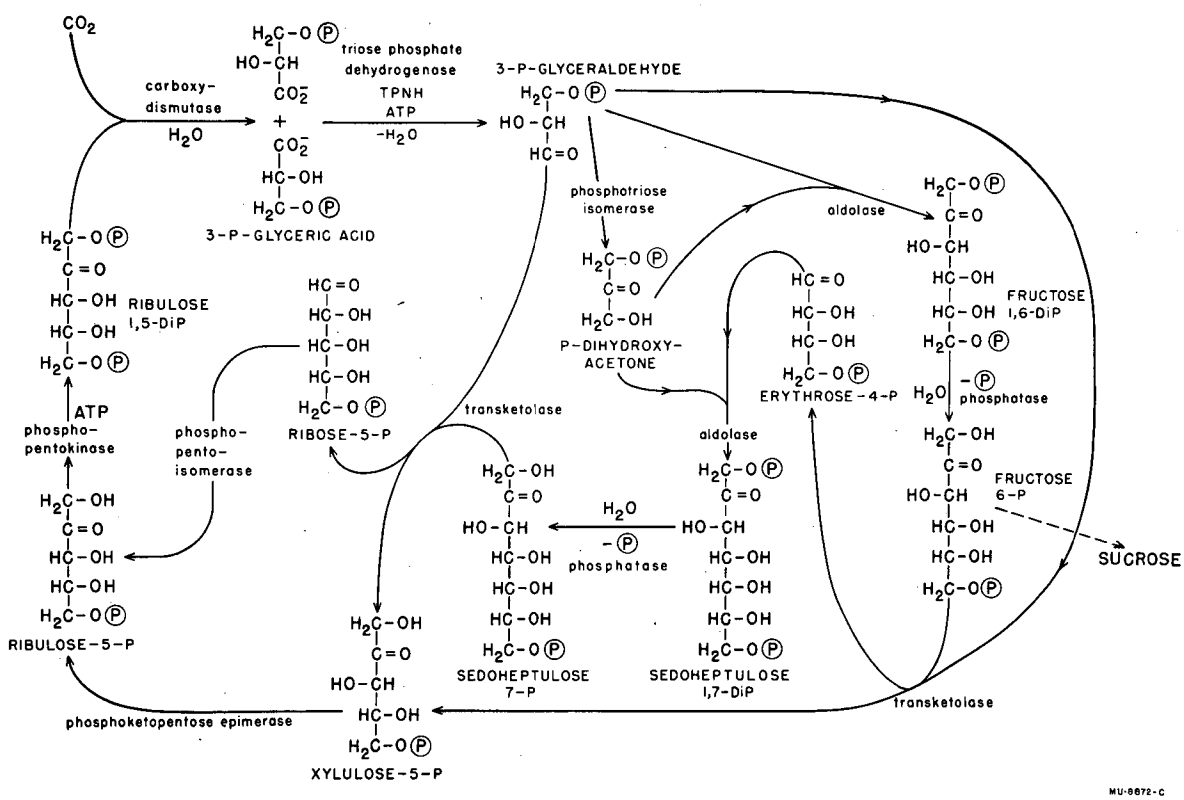

Fig. 4. The photosynthetic cycle.

The observation in this laboratory of R. Quayle (unpublished results) that little separation can be achieved between dihydroxyacetone phosphate and erythrose-4-phosphate on the normal two-way paper chromatogram was confirmed. In the search for tetrose and xylulose phosphates, attention was therefore concentrated on three adjoining areas containing mainly the triose phosphate ("T"), hexose cyclic phosphates ("G"), and ribulose-5-phosphate ("P"). A fourth area containing mainly ribulose diphosphate was also investigated.

The source of these radioactive areas was 24 two-way paper chromatograms of a combined 80% ethanol and 20% ethanol extract of Scenedesmus (30 ml of 1% cell suspension) which had been left for 1 hr to achieve a steady state with 1% CO_2 in oxygen and KH_2PO_4 (0.5 ml, 3.2×10^{-6} M), allowed to photosynthesize for 5 min with $NaHC^{14}O_3$ solution (0.9 ml, 360 μc), and then flushed with air (1 min).

After elution of the "T," "G," "P," and " diphosphate" areas, the sugar phosphates were incubated at 30° for 16 hr with purified phosphatase (freshly prepared from Polidase S by the method of R. Quayle - unpublished results).

Phosphatased "T" phosphate gave mainly dihydroxyacetone* together with traces of a tetrose (probably erythulose*--NOT erythrose), ribulose, and traces of sugar acids. Phosphatased "G" phosphate gave mainly glucose,* another hexose, glucose-1,2-cyclic phosphate, small amounts of ribulose, xylulose, and a trace of tetrose (probably erythulose--NOT erythrose). Phosphatased "P" phosphate gave ribulose,* xylulose,* dihydroxyacetone, hexoses, glucose-1,2-cyclic phosphate, and traces of sugar acids.

If an enlarged "G" phosphate area was taken it was possible after phosphatase action to demonstrate that all the tetrose was then concentrated in this area and that it did not co-chromatograph with erythrose. This area was also the most suitable for identifying xylulose after phosphatase action. Wherever dihydroxyacetone was detected the radioactivity appeared to coincide with the rear end of the spot. Phosphatased "diphosphate" area gave mainly ribulose,* some xylulose,* sedoheptulose, glucose, galactose, and traces of sugar acids. Only a minute amount of fructose* could be detected. A trace of a possible tetrose was also present.

In control experiments on the purity of the phosphatase used, incubation with ribose-5-phosphate gave only ribose (with no detectable ribulose); with erythrose-4-phosphate the spot obtained corresponded to erythrose (prepared by the action of ammonia on D-arabinose disulfone) and not erythulose.

Preliminary Studies on Some Unidentified Intermediates

Figure 5 shows the relative location of some unidentified intermediates detected on chromatograms obtained by the method described in the previous section. Following is a summary of the information so far obtained about them.

---

* Starred items were identified by co-chromatography.

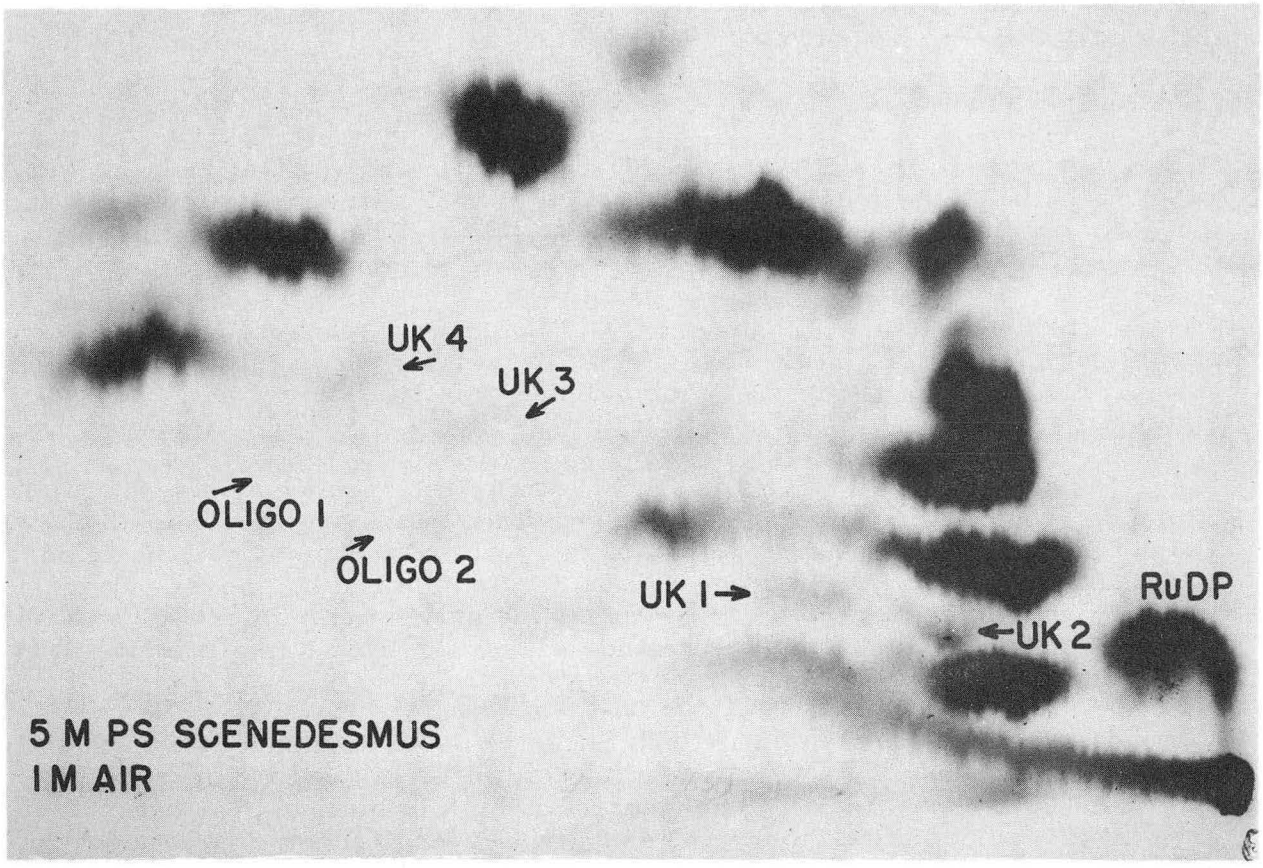

ZN-1451

Fig. 5. Some unidentified intermediates in Scenedesmus metabolism.

Unknown 1 (UK 1). The original spot absorbs light in the ultraviolet. When it was submitted to paper ionophoresis in sodium propionate the major component had a mobility just less than the sugar monophosphates; a minor component with a smaller mobility was also detected. Both components were negatively charged ions. After treatment with purified phosphatase, UK 1 gave only ribose and a component with an R_f value in phenol-water greater than that of erythrose.

Hydrolysis with N H_2SO_4 at 100° for 20 min and separation of the products in butanol-propionic acid showed:

(a) main component R_f 1.27 > adenosine (a purine or pyrimidine?);

(b) small amount component R_f = ribose;

(c) small amount component R_f < ribose.

Hydrolysis with 0.01 N H_2SO_4 at 100° for 10 min and separation of the products in butanol-propionic acid showed no (a), traces of (b) and (c), and the main activity concentrated in a spot R_f < (c). Components with even smaller R_f's were detected.

Unknown 2 (UK 2). Except that UK 2 has a smaller R_f value in phenol-water than UK 1, the observations recorded above for UK 1 were true for UK 2. This suggests a homologous relationship between the two compounds.

Unknown 3 (UK 3). When submitted to paper ionophoresis in sodium propionate one component had the same mobility as a sugar monophosphate and another might be a neutral component. After treatment with purified phosphatase, UK 3 gave only one radioactive compound having R_f = dihydroxyacetone in phenol-water and > dihydroxyacetone in butanol-propionic acid. Its position indicated that it was neither glyceraldehyde nor glycerol. It does, however, lie in the nucleoside region.

Unknown 4 (UK 4). When submitted to paper ionophoresis in sodium propionate, two components with very low mobilities (neutral?) could be detected. When treated with phosphatase (which is believed to contain several glycosidases) it gave traces of glucose and fructose presumably arising from a sucrose impurity in the original UK 4 together with two spots in the ribose-xylulose region and a third with a greater R_f in butanol-propionic acid.

Oligosaccharide 1 (Oligo 1). Oligo 1 is probably non-reducing since it did not form a benzylamine complex.[5] When hydrolyzed with 2 N H_2SO_4 at 100° for 4 hr it gave glucose and another component in the 5-carbon sugar region.

Oligosaccharide 2 (Oligo 2). Oligo 2 is also probably non-reducing since it did not form a benzylamine complex. When hydrolyzed with 2 N H_2SO_4 at 100° for 4 hr it gave glucose and a very small amount of another component in the 5-carbon sugar region.

---

[5] R. J. Bayly and E. J. Bourne, Nature 171, 385 (1953).

Maps have been prepared showing the relative positions of some sugar alcohols and some pyrimidines, purines, nucleosides, and nucleoside mono- and triphosphates when separated on the normal two-way paper chromatograms.

Future work will be directed towards the identification of the tetrose phosphate and attempts to identify the intermediate compounds discussed above. An experiment has already been commenced using P^{32}-phosphate to determine whether some of these unknowns indeed contain phosphate moieties.

RADIATION DECOMPOSITION OF CHLOROPHYLL AND HEMIN

Ann C. Kleerup and Bert M. Tolbert

The two metal porphyrins, chlorophyll and hemin, are common, respectively, to all photosynthesizing plants and to most vertebrate animals. Chlorophyll is very sensitive to visible and ultraviolet irradiation. Hemoglobin is, of course, a distinguishing compound of the hematopoietic system, one of the more radiation-sensitive parts of biological systems. Therefore, we are studying the effects of gamma irradiation on these compounds to provide fundamental information in radiation biochemistry. The first experiments are being done with pure dry air-free samples.

Hemin can be purchased as a fairly pure compound (97%). It has been recrystallized from a pyridine–glacial acetic acid–NaCl mixture to give spectrophotometrically pure material. Samples are being irradiated in the Co^{60} source in sealed tubes. They will be analyzed by several methods.

The problem of obtaining appreciable quantities of relatively pure chlorophyll a or b, or even a mixture of the two substances, is rather considerable. Commercial chlorophyll is largely pheophytin. Some chlorophyll has been obtained by acetone extraction of dried fresh spinach leaves followed by chromatography on powdered sugar (grocery store type, 3% starch). A solution of the chlorophyll in petroleum ether is placed on a column of powdered sugar and the chromatogram developed with a mixture of equal volumes of benzene and petroleum ether. When the separation is fairly complete, the column is cut into sections of blue-green chlorophyll a, gray-green chlorophyll b, and a band which is a mixture of the two. The chlorophyll from each band is eluted with dry ethyl ether, the ether evaporated off, and the chlorophyll rechromatographed. Then the pure chlorophyll obtained in this manner is eluted with dry ethyl ether. The solution is dried with anhydrous Na_2SO_4, filtered, and evaporated to dryness at room temperature under slightly reduced pressure or with a stream of dry nitrogen. Only 5 mg of spectrophotometrically pure chlorophyll b has been obtained, and this is tarry rather than a nice crystalline solid, probably because of the microcrystalline character of the chlorophylls.

EFFECTS OF IONIZING RADIATION ON CHOLINE ANALOGS

Richard M. Lemmon, Peggy Kwong, and Margaret A. Parsons

A problem of particular interest in the present studies of the radiation sensitivity of choline analogs is to determine the effect on this sensitivity of the presence of a proton-attracting anion in a choline salt. It is known from work on the thermal decomposition of quaternary ammonium salts and bases (Hofmann degradation) that such an anion increases the ease of thermal degradation. It was therefore conceivable that choline acetate, $[(CH_3)_3NCH_2CH_2OH]^+CH_3CO_2^-$, might be even more radiation-sensitive than choline chloride, $[(CH_3)_3NCH_2CH_2OH]^+Cl^-$, since the acetate ion has a far greater proton affinity than is exhibited by chloride ion or by any of the other anions of choline salts with which we have hitherto worked. In order to investigate this possibility we have synthesized analytically pure choline acetate and have subjected the anhydrous crystalline salt, under high vacuum, to the γ radiation of the Co^{60} source. The conditions under which the irradiations were performed, and the analytical procedures (reineckate analysis) used to determine the extent of radiation decomposition, are exactly those which were described in an earlier report.[1] Three γ irradiations have been carried out. The amounts of radiation received by the samples were 7.7×10^7, 9.2×10^7, and 9.2×10^7 rep, respectively, and the corresponding percentages of decomposition and G values (molecules decomposed/100 ev) are: 11% (G = 10), 17% (G = 13), and 13% (G = 10). It therefore appears that the degree of proton affinity of the anion plays no decisive role in altering radiation sensitivity in the choline series.

Methoxide ion, CH_3O^-, has an even greater affinity for protons than does acetate ion. We have therefore attempted to prepare choline methoxide, $[(CH_3)_3NCH_2CH_2OH]^+CH_3O^-$, by reacting choline chloride with sodium methoxide in absolute methanol. We have been unable to obtain any appreciable quantities of choline methoxide, however, and have therefore been unable to study the radiation sensitivity of this compound.

1 Richard M. Lemmon and Margaret A. Parson, UCRL-2647, July 8, 1954, p. 4.

PREPARATION OF CALCIUM GLYCOLATE FOR RADIATION-SENSITIVITY STUDIES

Irville M. Whittemore and B. M. Tolbert

A sample of calcium glycolate labeled with carbon-14 was found by Weinhouse[1] to be relatively unstable with time. This unusually large decomposition was presumed caused by radiation and was therefore checked with γ and e^- irradiation in this laboratory by Grisebach.[2] No unusual radiation effect was found in these experiments. Thus, the decomposition observed by Weinhouse may be due to storage conditions, or to specific effect of the C^{14}-radiation. This question is being resolved as follows:

Calcium glycolate-1-C^{14} has been prepared on a millimole scale with a specific activity of about 1.5 mc/mM. The method of preparation was that which has been described by Hughes and Tolbert.[3] The products were reduced to the anhydrous state by drying in vacuo in a drying pistol at 100° C.

The calcium glycolate was recovered in three batches: (a) the first crop, (b) a batch recrystallized from the first crop, (c) a batch crystallized from the combined mother liquors and washes of (a) and (b).

The purity of the three batches was checked by two-dimensional paper chromatography. The solvents were n-butanol saturated with 0.5 N NH_4OH and a mixture of ethanol, water, and 15 N NH_4OH in the ratio of 82:15:3. All three batches showed only one radioactive spot together with about 2% of the radioactivity still on the origin.

Two of the spots from the chromatograms were eluted with H_2O and rerun. One was run in the same manner as before, using warm air to dry the liquid on the paper. This paper also showed 2% of the radioactivity on the origin after being run. The other spot was redried on the paper without the use of heat and showed only 1% of the activity on the origin after chromatographing. This strongly indicates that the original calcium glycolate was pure and that the 2% activity on the origin was the result of placing the glycolate on the paper and drying it.

In addition to the calcium glycolate of 1.5 mc/mM, another batch of much lower activity (0.02 mc/mM) was also prepared. Its purity was comparable to that of the more radioactive samples.

Several portions of all four batches of glycolate were sealed in vacuo in glass tubes. The remainder of the salts were stored in ordinary glass weighing bottles.

The purity of the sealed ampoules will be checked in a year or more. It is hoped that the relative purity of the samples after storage will indicate whether or not radioactive calcium glycolate is subject to more than ordinary self-decomposition.

---

[1] See B. M. Tolbert et al., J. Am. Chem. Soc. 75, 1867 (1953).

[2] H. Grisebach, UCRL-3068, July 6, 1955, p. 28.

[3] D. M. Hughes and B. M. Tolbert, UCRL-256 (1948).

Calvin

PARTITION CHROMATOGRAPHY OF CARBON DIOXIDE

Patricia T. Adams and Bert M. Tolbert

The possibility of an isotope effect in the chromatography of oxygen-containing compounds is under investigation. It is hoped that, if such an effect is discovered, it can be utilized as a source of oxygen-17-enriched compounds.

The partition chromatography of gaseous carbon dioxide, with nitrogen as the eluting gas, is being studied. Preliminary experiments were performed using carbon-14 dioxide as a tracer and analyzing the eluent gas by means of a 10 cc ionization chamber. A continuous recording of the amount of radioactivity in the gas stream was thus obtained.

The absorbent for the chromatographic columns was prepared by mixing Celite with half its weight of the liquid to be used as the stationary phase. This mixture was packed uniformly in long glass tubes of 3 mm inner diameter. Uniform packing was achieved by mounting the glass tube on a vibrating motor and adding the absorbent slowly, with intermittent tapping to pack loose particles.

Carbon-14 dioxide (3 mg) was injected onto a column 3 mm by 4 ft with n-butyl carbitol as the stationary phase. Nitrogen was passed through the column at 18 cc/min. The carbon dioxide emerged as a concentrated band very soon after injection, showing that there was little, if any, absorption on the column.

It was hoped that repeated passage through the column might produce the maximum possible chromatographic effect. A circulating pump was installed in the system to allow the eluent gas to be reapplied to the top of the column. However, because the construction of the circulating pump resulted in mixing of rather large volumes of eluent gas, the carbon dioxide became diffused uniformly throughout the system after only a few cycles.

In another experiment, acetone was chosen as the stationary phase because of the high solubility of carbon dioxide in acetone at low temperatures. A column 3 mm by 16 ft was used. The column was cooled by submersion in a vessel packed with dry ice. Carbon-14 dioxide (2 mg) was injected onto the column and nitrogen was swept through the system at a rate of 10 cc/min. The carbon dioxide emerged in a smooth sharp peak after 14 min. Likewise, on a column 3 mm by 32 ft, with a nitrogen flow rate of 4 to 5 cc/min, the carbon dioxide emerged in a very similar peak pattern after 40 min. These time intervals indicate that appreciable absorption does take place on the column when the stationary phase is acetone at dry ice temperatures.

The size of the ionization chamber (10 cc) and its resulting mixing of a relatively large volume of gas is believed capable of obscuring any small separation effect obtained on the column. An isotope effect during chromatography would probably result in the emergence of the carbon dioxide as an unsymmetrical peak with perhaps a small plateau on the descending slope. Thus, it is important that the instrument used for analysis have a minimum mixing volume so that resolution of the shape of the curve be very good.

A thermal conductivity cell is currently being assembled. Carbon dioxide may be determined in small concentrations with this apparatus by the change in thermal conductivity of the eluent gas. The gas from the column will go through the analysis unit in small-bore tubing so that chances for mixing are minimized. In this way it is hoped that the fine structure of the elution curve may be seen.

THE RESOLUTION OF DL-VALINE

Patricia T. Adams

Several synthetic DL-amino acids labeled with carbon-14 are being resolved. The procedure used is based upon the method of Price, Gilbert, and Greenstein.[1] It utilizes the ability of hog kidney acylase to hydrolyze acyl-L-amino acids while leaving acyl-D-amino acids untouched. The preparation described below, using unlabeled DL-valine, shows the method of resolution to be adaptable to the small scale necessary for use with the labeled material.

Chloracetyl Valine

DL-valine (0.76 g, 6.5 millimoles) was dissolved in a small volume of 4 N sodium hydroxide. The solution was cooled in an ice bath and stirred while 1.5 ml of chloracetyl chloride was slowly added. Additional 4 N sodium hydroxide was added intermittently to keep the solution basic. After the addition was complete, the solution was stirred at room temperature for 30 min. The reaction solution was acidified to pH 3 with 6 N hydrochloric acid and extracted continuously with ether for 4 hours. The ether solution was washed with water, dried with sodium sulphate, and evaporated to dryness at room temperature *in vacuo*. The residue was triturated 6 times at room temperature with petroleum ether to remove chloroacetic acid. The trituration leaves behind solid chloracetyl valine. Chromatographic analysis showed the product (515 mg, 2.7 millimoles) to be free from contamination with valine.

The non-acylated valine remains in the aqueous layer of the extraction. It may be recovered in pure form, since the only contaminant present is sodium chloride. In this experiment the valine was not recovered, however, so that the yield has not yet been determined.

Hydrolysis of Chloracetyl L-Valine

The chloracetyl-DL-valine was dissolved in water and the pH adjusted to 7.6. Hog kidney acylase (15 mg; obtained from Armour Co., Chicago, Ill.) was added to the solution, the pH re-adjusted, and the volume made to 25 ml. This solution was incubated at 37° C for 4 hours. At that time, 15 mg additional enzyme was added and the solution maintained at 37° C for 16 hours. The pH of the digestion solution was then adjusted to 5 with acetic acid and the solution stirred with charcoal for 2 hours to remove protein. After filtration, the clear solution was evaporated to a very small volume *in vacuo* at room temperature. Care must be taken against chemical hydrolysis of the unhydrolyzed acyl-D-valine.

---

[1] V. E. Price, J. B. Gilbert, and J. P. Greenstein, J. Biol. Chem. 178, 503, 179, 1169 (1949).

L-Valine

The digested solution was applied to a Dowex-50 cation exchange column in the hydrogen form. Slow rinsing with 250 ml of distilled water removed the acyl-D-valine quantitatively from the column. The L-valine was eluted with 200 ml of 2 N hydrochloric acid. The acid solution was evaporated to dryness in vacuo. The residue was dissolved in a minimum quantity of absolute ethanol, chilled in ice water, and treated with a stream of ethylene oxide for 20 min. The precipitated L-valine was collected on a filter, washed with alcohol, and dried. It weighed 95 mg. Specific rotation: α_D(in 6 N HCl), 22; theory, 27.4.

D-Valine

The effluate fraction from the Dowex-50 column was evaporated to dryness and treated with 2 N hydrochloric acid under reflux for 4 hours. The hydrolysis solution was then evaporated to dryness and the amino acid was precipitated from alcohol solution with ethylene oxide as described above. Eighty-five mg of D-valine was isolated. α_D, -23.6; theory, -27.1. The combined recovery of resolved valine was 180 mg (1.54 millimoles) or 57% yield from chloracetyl valine.

SYNTHESIS OF GLYCINE-2-C^{14} VIA AN IMPROVED METHANOL-C^{14} PREPARATION

Ann C. Kleerup and Patricia T. Adams

A preparation of glycine-2-C^{14} was undertaken by the following steps:

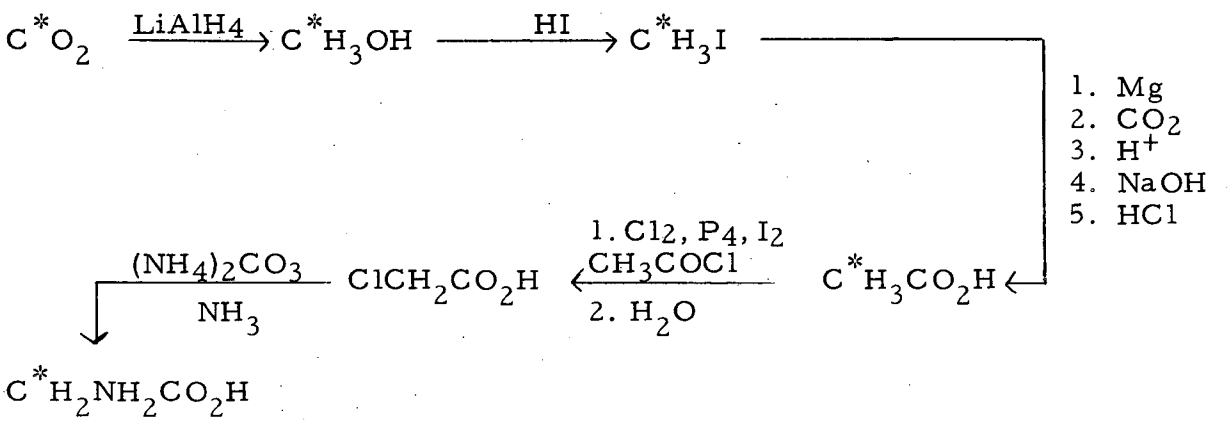

The procedures used, except for the methanol preparation, were those previously published.[1, 2] Since preparation of the solution of $LiAlH_4$ in tetrahydrofurfuroxytetrahydropyran (TFTP) ordinarily used for the reduction of CO_2 to CH_3OH is laborious and time-consuming, an attempt was made to do the reduction by using a slurry of $LiAlH_4$ in the same solvent. This single modification, however, led to a 38% yield of CH_3I from the $BaCO_3$ instead of the 80% yield usually obtained by using the solution for reduction. Several other reductions of CO_2 under different conditions were run and the following procedure for slurry reduction was determined as satisfactory. $LiAlH_4$ was powdered with mortar and pestle in a dry atmosphere, and then a slurry of about 1.15 g of this powdered $LiAlH_4$ (about 100% excess for 15 mM of CO_2) in 50 ml TFTP was stirred 5 hours at 60° in a dry helium atmosphere. Then the slurry was transferred to the vacuum line and 15 mM of prepared $C^{14}O_2$ was stirred into the mixture. The mixture was frozen in liquid nitrogen and the remaining CO_2 distilled into the flask. The mixture was thawed quickly and then stirred 1/2 hour at room temperature and for 1 hour at 55° to 60°. The mixture was then swept in the usual manner to isolate $C^{14}H_3OH$, which was converted to iodide. The yield of CH_3I from $BaCO_3$ by this procedure was 82.5%.

This methyl-C^{14} iodide was converted to sodium acetate in 79% weight yield. The acetate was converted to glycine-2-C^{14} in 69% weight yield to give an over-all radioactive yield from $C^{14}O_2$ of 30%. In this manner 0.760 g of glycine of specific activity 11.8 μc/mg was prepared. Anal. Calcd. for $C_2H_5NO_2$:C, 32.0; H, 6.7; N, 18.7. Found: C, 32.1; H, 6.89; N, 18.4. Two-dimensional chromatography (a) propanol-H_2O; (b) butanol–propionic acid–H_2O) on Whatman No. 1 paper gave only one spot. A fraction from the ion-exchange elution containing mostly iminodiacetic acid-2-2-C^{14} (a product of the synthesis) was saved but not purified (weight 0.0490 g).

---

[1] R. Ostwald, J. Biol. Chem. 173, 207 (1948).

[2] D. E. Pack and B. M. Tolbert, UCRL-1957 (1952)

PREPARATION OF DL-CARNITINE HYDROCHLORIDE

Franco Mazzetti and Richard M. Lemmon

A brief account was given in an earlier quarterly report[1] of the synthesis of carnitine hydrochloride. This compound, $[(CH_3)_3NCH_2CH(OH)CH_2COOH]^+Cl^-$, which is also known as vitamin B_T, is of interest to us as it is one of a series of quaternary ammonium salts whose radiation sensitivities are under investigation. Since our earlier report we have re-investigated the synthesis of carnitine with the object of simplifying and improving the synthetic procedures that are in the literature. The reactions we have employed, and the yields obtained, are as follows:

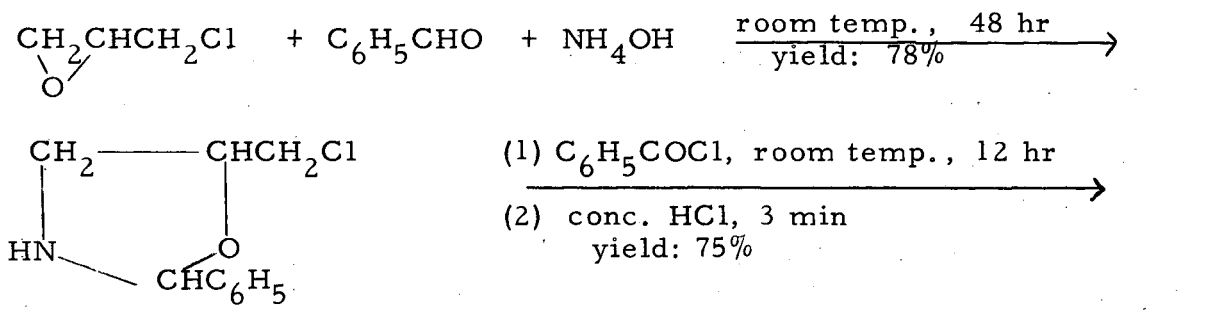

$[(CH_3)_3NCH_2CH(OH)CH_2COOH]^+Cl^-$.
carnitine hydrochloride

The last step in the reaction sequence, the methylation of the 4-amino-3-hydroxybutyric acid, is a particularly troublesome one. The presence of hydroxyl ions, which is necessary to effect the methylation of the nitrogen atom, also promotes the formation of the lactam of the amino acid. The best yields so far obtained have been by the use of the Dowex-2 anion-exchange resin as a source of hydroxyl ions. Further research is in progress to try to improve the yield at this step.

---

[1] Richard M. Lemmon, Franco Mazzetti, and Margaret A. Parsons, UCRL-3068, July 6, 1955, p. 25.

LIQUID SCINTILLATION COUNTING OF TRITIUM BY MEANS OF COINCIDENCE TECHNIQUES

Elton M. Baker and Fred Vogelsberg

The detection of tritium, which emits beta particles having a maximum energy of 18 kev, necessitates departure from the usual counting methods. Ion chambers, proportional counters, or Geiger counter arrangements are sensitive, but involve the chemical conversion of samples containing tritium into hydrogen gas or some other gaseous substance, with the possibility of dilution and isotope fractionation which results in large errors. The use of liquid scintillation counting techniques provides a sensitive method utilizing samples of radioactive compounds in the form of water or solutions and suspensions, which provide nearly 100% counting geometry.

A limitation of the scintallation counter is that noise inherent in the photomultiplier tubes or electron tubes in the amplifier is of the same order of magnitude as the electrical pulse that results when beta energy is converted by a phosphor, emitted as light and detected by the photomultiplier tube. These energy-conversion processes become very important in the detection of tritium disintegrations. Consideration must be given to the fact that with the liquid phosphors presently available the low beta energy from tritium may not be converted to light energy with complete linearity, and a diffuse spectrum results.

Although the sensitivity of the photomultiplier tube is dependent on the coating of the light-sensitive cathode and its ability to eject a photoelectron, the final detection is determined in large part by the collection efficiency and the amplification of the photoelectric pulse. An increase of potential across the dynodes in the photomultiplier tube will provide increased amplification not only for the photoelectron ejected but also for spurious electrons. With higher than optimum photomultiplier dynode voltages the photomultiplier output is increased, but signal-to-noise ratio is not improved and there is evidence of increasing numbers of afterpulses, resulting from gas ions' impinging on the photocathode. This may be partially reduced by operation of the tubes at cold temperatures. Other electrical pulses may result from radioactive impurities, such as K^{40}, in the glass of the tube, and other source impurities in the metal surrounding the tubes.

In order to eliminate to a great extent these pulses which would otherwise be counted, a system of two tubes in coincidence has been devised. This means that counting will take place only when both tubes are affected simultaneously by light from a scintillating source or be accidentally coincident noise pulses occurring simultaneously in both photomultiplier tubes. The gain required to operate a coincidence system and pulse-height analyzer must be provided by the photomultiplier in its optimum voltage range followed by a vacuum-tube amplifier to supply the remainder of the gain needed. A minimum coincidence acceptance level is established to minimize noise background and the feedthrough of "single" overload pulses. The effects of external radiation may be further reduced by using a "window" discriminator in the analyzer. With proper adjustment, then, of pulses due to radiation from tritium amplified by means of properly chosen gains

of the photomultiplier tubes and amplifiers, the total number of individual tritium disintegrations accounted for may be better than 50%, which would be those energies between approximately 4 kev and 18 kev with as few as 400 accidental and background counts per minute. With gains adjusted to low levels and so that 30% of the disintegrations detected are between 6 kev and 18 kev, the total background count may be as low as 200 counts per minute.

In order to achieve the greatest counting efficiency and to hold background counts to a minimum, selected low-noise photomultiplier tubes of high photocathode sensitivity, and linear amplifiers with good overload characteristics, are employed.

The electronic system as shown in the block diagram (Fig. 6) of this counter is a dual channel coincidence analyzer comprised of two photomultipliers, each followed by preamplifiers, high-gain linear amplifiers, coincidence, and gating units, and finally the pulse-height analyzer.

Two DuMont 6292 photomultipliers with preamplifiers, mounted coaxially in a lighttight magnetically shielded housing within a refrigerator and viewing a thin sample at each face of the tube, provide an optimum geometrical arrangement. This apparatus was described in an earlier report.[1] Each preamplifier is a three-tube cathode follower output feedback loop with a gain of four. The preamplifier outputs are positive tail pulses of approximately 10 μsec time constant, connected to 120-ohm variable attenuators at the linear amplifier inputs through 6 feet of RG-62-μ cable. The high-voltage supply to each photomultiplier divider may be individually adjusted to equalize the gain of each channel.

Each linear amplifier is a modified Model III UCRL amplifier. There are three feedback loops, each stabilized by negative feedback, followed by twin cathode-follower output stages. They were modified to provide delay-line clipping at the input of the first loop and again at the input to the second loop. The effect is to provide equal and opposite polarity excursions to the second loop for each input tail pulse and thus reduce the paralysis effects of overload signals on the latter stages of the amplifier. The last amplifier loop employs a "bootstrap" feedback circuit to improve large-signal linearity and to extend the range of usable output.

The linear amplifier characteristics are:

Input: 120 ohm, 10 μsec positive tail pulses.
Gain: approximately 3000 maximum.
Output: Positive 0.05 μsec rise, 0.08 μsec fall, and 0.3 μsec pulse duration.
Amplitude: 80-volt maximum output when terminated in 1000 ohms impedance.
Noise: Less than 0.5 volt, and approximately 1 volt including preamplifiers.
Overload: Less than 5% base line supression after 2 μsec if not overloaded more than 30 times at full gain.
The output utilized is from 3 volts to 60 volts.

[1] Elton M. Baker, UCRL-2841, January 10, 1955, p. 17.

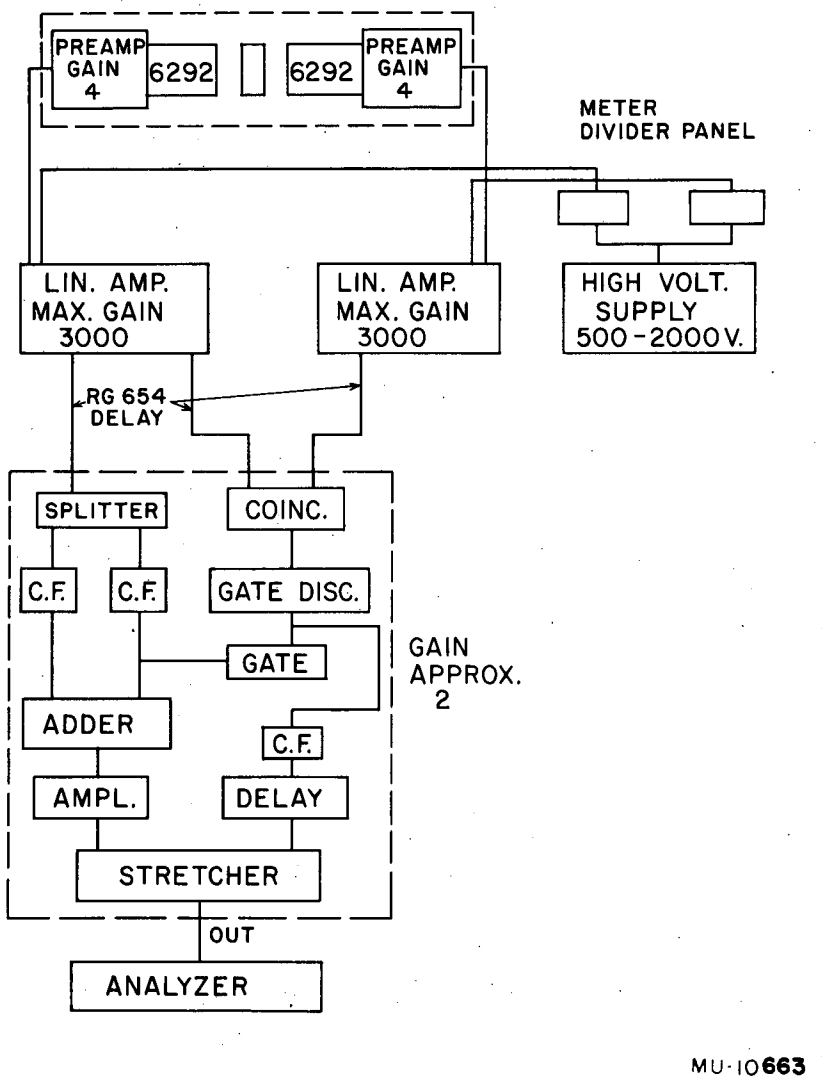

Fig. 6. Block diagram of coincidence counting system with pulse-height analyzer.

Two outputs are taken to the coincidence gate unit from the linear of the first channel: a signal pulse and a coincidence pulse; the latter pulse combined with a similar coincidence pulse. The latter pulse combined with a similar coincidence pulse from the second channel gates through only the signal pulses seen by both channels within the resolving time of the coincidence circuit (between 0.2 and 0.3 μsec). The coincidence inputs are limited to 60 volts by crystal-limiter and cathode-follower stages which drive a biased diode crystal coincidence circuit. The coincidence output triggers a 0.3-μsec univibrater biased to accept the minimum signal required to provide a 5-volt signal output without feedthrough of overload single pulses. The circuit of the coincidence unit is shown in Fig. 7.

True coincidence signals are linearly gated in the following manner: The input signal is attenuated by a factor of 2/3 (to relatively increase the coincidence signals) and limited at 45 volts maximum to assure operation of the signal selector in its linear range. The signal is split by an inverter stage into equal positive and negative signals. Compensation is provided so that the signals may be balanced to less than 1% in amplitude and shape at the output. From the inverter the opposing polarity pulses are fed to isolation cathode followers, which are coupled to a single-stage parallel feedback adder. Unless a coincidence occurs this is the desired effect. When there is a coincidence, however, a gating circuit supplies cathode current to the cathode follower of one of the opposite-polarity branches and in effect the signal of that polarity is moved down to the base line so that it no longer subtracts from the signal in the other branch, which passes through the adder unchanged. The operation of this "negativistic" gating circuit is such that gate feedthrough and distortion of the selected signal are eliminated so as to provide a more nearly linear gate.

An adjustable-gain feedback loop provides the final amplification to cover the range of the following pulse-height analyzer. The gate univibrator also operates a stretching circuit which widens the output pulse from 0.3 to 1 μsec, providing a clean constant with input to the analyzer discriminator. The output range is from 5 to about 110 volts. The input signal and coincidence pulses are properly phased by lengths of RG 65-μ cable between the linear amplifier and the coincidence gating unit.

Auxiliary equipment includes a calibration decade tail pulser to check the over-all gain and coincidence-level stability from the linear amplifier input through to the analyzer discriminator. The common high-voltage supply is monitored by a potentiometer and recorder. Standard samples and blank samples provide a check on over-all stability and background. In normal operation the gain following the photomultipliers is about 6000 and the high-voltage operating range is from 800 to 1300 volts depending upon the sample. Under these conditions the normal dead time is not greater than 5 μsec.

The most serious problems still remaining are afterpulsing in the photomultipliers at high voltage, stretching and base line overshoot in the linears at overloads greater than 30 times, and general poor resolution of the organic phosphors. The photomultipliers were selected from those available for best signal-to-noise characteristics. They are unfortunately older tubes with mica shield support structure, which does not permit

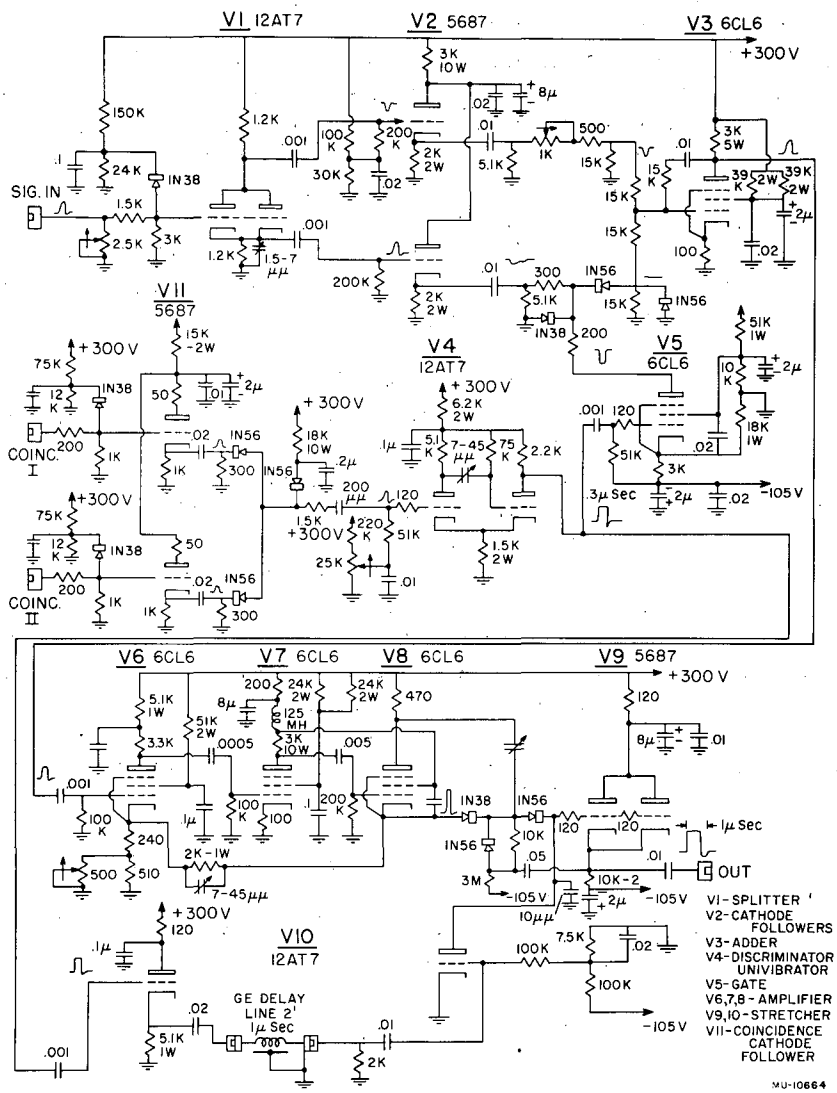

Fig. 7. Coincidence gate unit.

adjustment of shield potential to obtain optimum resolution. Both the satellite pulsing and linear amplifier overload response impose a limit on the gain that may be obtained from the phototubes. For each sample type the high voltage must be limited to the "plateau" region for accuracy of results and sometimes at a sacrifice of maximum counting efficiency.

The problem of preparing a suitable liquid scintillator has been discussed in previous reports;[2] however, recently two major improvements have been made over the customary ethanol-toluene-water solution. Comparisons of the effect of methyl alcohol, ethyl alcohol, n-propyl alcohol, and isopropyl alcohol indicate that less quenching of the energy-transfer process may be had by using isopropyl alcohol, providing a counting efficiency of 25%. Methyl alcohol has a greater quenching effect and n-propyl and ethyl alcohol have about the same effect, as indicated in Table II. Care must be taken in all cases to provide a completely miscible mixture at the counting temperature of -17°C. A sample of tritiated water from the Atomic Energy Project at Chalk River, Canada, was used as a standard to provide a comparison of counting efficiencies.

A major disadvantage to any of the above solutions is that only a small amount of tritiated water may be used without producing a two-phase system. This disadvantage has been partially overcome by using acetic anhydride, which is hydrolyzed by the tritiated water. Ten percent more acetic anhydride is used than is needed to completely utilize the water. This sample is then placed in the scintillation solution. The latter solution consists of 5 g diphenyloxazole dissolved in 1 kg of redistilled and purified toluene free from impurities and gases. Although a greater effect of quenching is observed because of the acetic acid and the observed efficiency of counting is only 10%, the reduced pulse size of the electric signal from the photomultiplier tube is partially overcome by raising the high voltage across the dynodes. The over-all gain from use of a sample of water that is eight times as large provides a much more effective scintillating solution for samples of lower activity.

Preliminary trials using propionic anhydride indicate that there is less quenching than with acetic anhydride. Work will continue with other scintillation solutions and systems, and it seems probable that a greater increase in counting efficiency may be expected.

---

[2] Elton M. Baker, UCRL-2932, March 30, 1955, p. 46; UCRL-3068, July 6, 1955; J. Phys. Chem. 59, 1182 (1955).

Table II

Scintillation counting efficiency for tritium in several alcohol-toluene solutions

Run No.	Volume of Toluene-Phosphor Solution (ml)	Solvating Medium	Calc. Dis. rate/min	Observed cts/min	Efficiency
1	6.7	1 ml isopropanol	194,800	49,900	25.6%
2	6.7	1 ml toluene	106,800	27,400	25.7%
3	6.7	1 ml ethanol	106,800	18,800	17.6%
4	6.7	1 ml n-propanol	106,800	20,800	19.5%
5	6.7	1 ml isopropanol	106,800	23,000	21.5%
6	6.7	1 ml methanol	106,800	16,100	15.0%
7	6.0	1.3 ml acetic anhydride	155,500	24,000	15.4%
8	6.3	0.75 ml propionic anhydride	77,900	15,300	19.6%

* 25-λ samples of tritiated water were used in No. 1; No. 2 does not contain water; all others contain 25 λ of dead water except in 7 and 8, where 200 λ and 100 λ of tritiated water were used, respectively. Numbers 2, 3, 4, 5, and 6 contain a known trace of high-specific-activity tritiated benzoic acid.

LIPOGENESIS IN THE ADIPOSE TISSUE OF THE INTACT RAT

Richard M. Lemmon, Samuel Lepkovsky, and Margaret A. Parsons

In collaboration with the Department of Poultry Husbandry we have undertaken some research designed to aid in our understanding of the biochemical mechanisms involved in hunger and satiety. In particular, we wished to measure the effect, if any, of the ingestion of food on the rate of lipogenesis or fatty acid synthesis, in the fat depots (adipose tissues) of the animal body. For this purpose we obtained a colony of rats that were trained to eat their entire daily food supply in two hours. Some of the rats were sacrificed prior to feeding (after 24 hours' fasting) and others at 2, 5, or 9 hours after feeding. In all cases, 2 hours before the animals were sacrificed they received an intraperitoneal injection of a solution of sodium acetate-2-C^{14}. After the animals were sacrificed, the livers and fatty tissues were cut out and the fatty acids were isolated by the procedure of Felts, Chaikoff, and Osborn.[1] The fatty acids were dissolved in warm, 1 N NaOH solution; aliquot portions were pipetted into platinum dishes and the solution was evaporated to dryness under a hot-air blower. The specific activities were then determined by means of a windowless flow-type counter.

The fasted rats showed very low lipogenic activity in the adipose tissue (mesenteric, renal, retroperitoneal, and subcutaneous fats) and comparatively high activity in the liver. High peaks of lipogenic activity were observed in both the liver and the adipose tissue 2 and 5 hours after the cessation of feeding. The rate of fat synthesis in the tissues seemed to depend greatly on how much time had elapsed since feeding, but not on the amount of food taken into the stomach.

While the highest average specific activities were observed in the liver, the greatest increases in specific activity (2000% to 4000% above that in the fasting state) were observed in the adipose tissues. The corresponding increase in the liver specific activities was 200% to 600%. The great increases in specific activity of the fatty acids in the adipose tissues clearly indicate that these tissues are very active sites of lipogenesis during the disposal of ingested food. It is still possible, however, that the bulk of the labeled fatty acids were rapidly synthesized in the liver and transported to the fat depots. This possibility is being investigated.

---

[1] J. M. Felts, I. L. Chaikoff and M. J. Osborn, J. Biol. Chem. 191, 683 (1951).

RESPIRATORY METABOLISM OF ACETATE, GLUCOSE, AND GLYCINE IN THE HEREDITARY OBESITY-DIABETES SYNDROME OF MICE

Ann M. Hughes, B. M. Tolbert, and Denham Harmon

The strain of mice, developed at Bar Harbor, which exhibits a hereditary obesity-diabetes syndrome has been rather extensively studied. A concise review of this work is presented by Guggenheim and Mayer.[1] They also report, in the same paper, studies on acetate metabolism in this strain of mice, reporting a decreased production of $C^{14}O_2$ from labeled acetate over a three-hour period, and suggesting a partial block of the C_2 fragment oxidation as the characteristic biochemical lesion in these animals. Parson and Crispell[2] present data that do not confirm those of Guggenheim and Mayer.

Mayer, Bates, and Dickie[3] report a high blood-sugar level in these obese mice: 200 mb % compared to 110 mg % for the nonobese controls. Fasting for 4 hours lowered the blood-sugar level of the obese mice 50% to 60%, while the controls remained unchanged. The obese mice also proved to be very insulin-resistant.

With this background it was felt that interesting and valuable data on these animals could be obtained by use of our breath-line apparatus, previously reported.

Obese mice, both male and female, and their litter-mate controls were obtained from the Jackson Memorial Laboratory, Bar Harbor, Maine. Acetate-2-C^{14}, glucose-C^{14}_6, and glycine-2-C^{14} were the compounds tested. In each case the dose, injected either intraperitoneally (i.p.) or intravenously (i.v.) was 1 mg (about 5 μc). Respiratory metabolism was followed for 7 hours. In some experiments involving the metabolism of glucose the animals were starved 24 hours prior to the experiment. Results are shown in Figs. 8 through 15.

The first experiments, in which acetate was injected i.p., showed a striking difference between the obese and control animals (Figs. 8, 9). It was felt that, owing to the great quantity of fatty tissue in the abdominal cavity of the obese mice, the differences seen in respiration could be caused entirely by a slower absorption of the injected acetate. Therefore the experiments were repeated, injecting the acetate i.v. instead of i.p.[4] The same type of recovery curves, only higher, were obtained (Figs. 10, 11). Our data, therefore, not only confirm those of Guggenheim and Mayer, but show the respiratory metabolism of acetate over a period more than twice as long as the three-hour period reported by them. The lack of agreement

---

[1] K. Guggenheim and J. Mayer, J. Biol. Chem. 198, 259 (1952).

[2] W. Parson and K. R. Crispell, Metabolism 4, 227 (1955).

[3] J. Mayer, M. W. Bates, and M. M. Dickie, Science 113, 746 (1951).

[4] We are indebted to Martha Kirk for the intravenous injections.

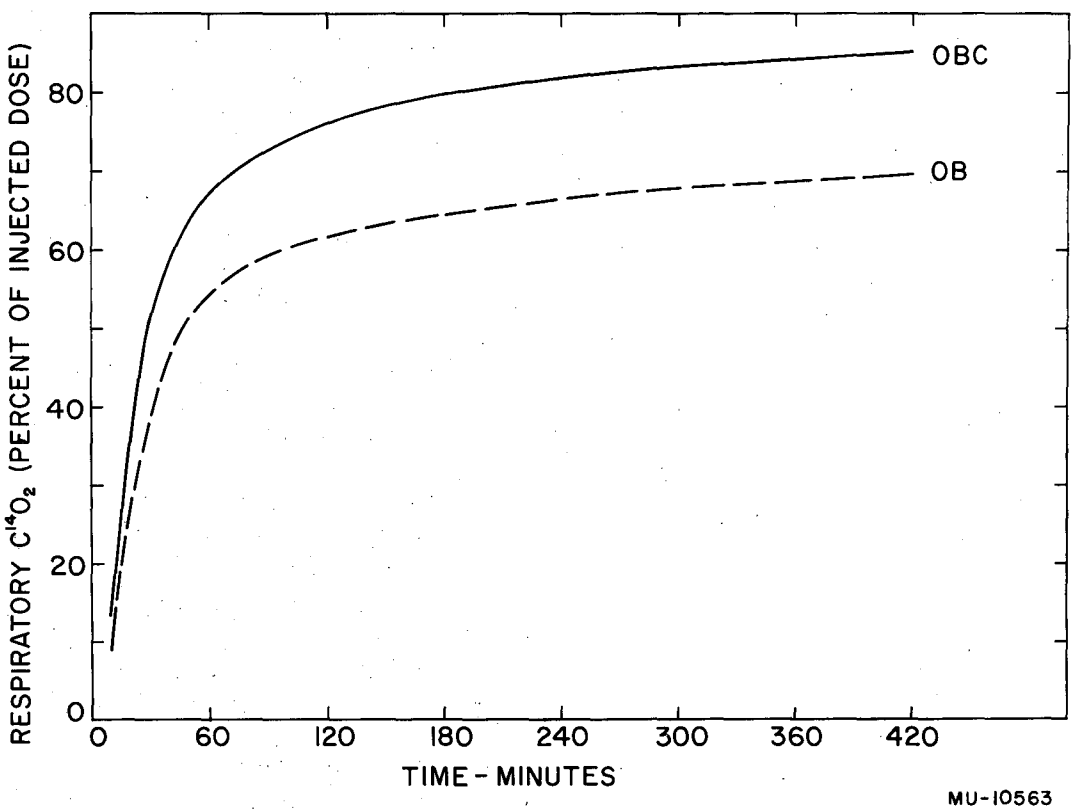

Fig. 8. Cumulative excretion of sodium acetate-C^{14} injected i.p.

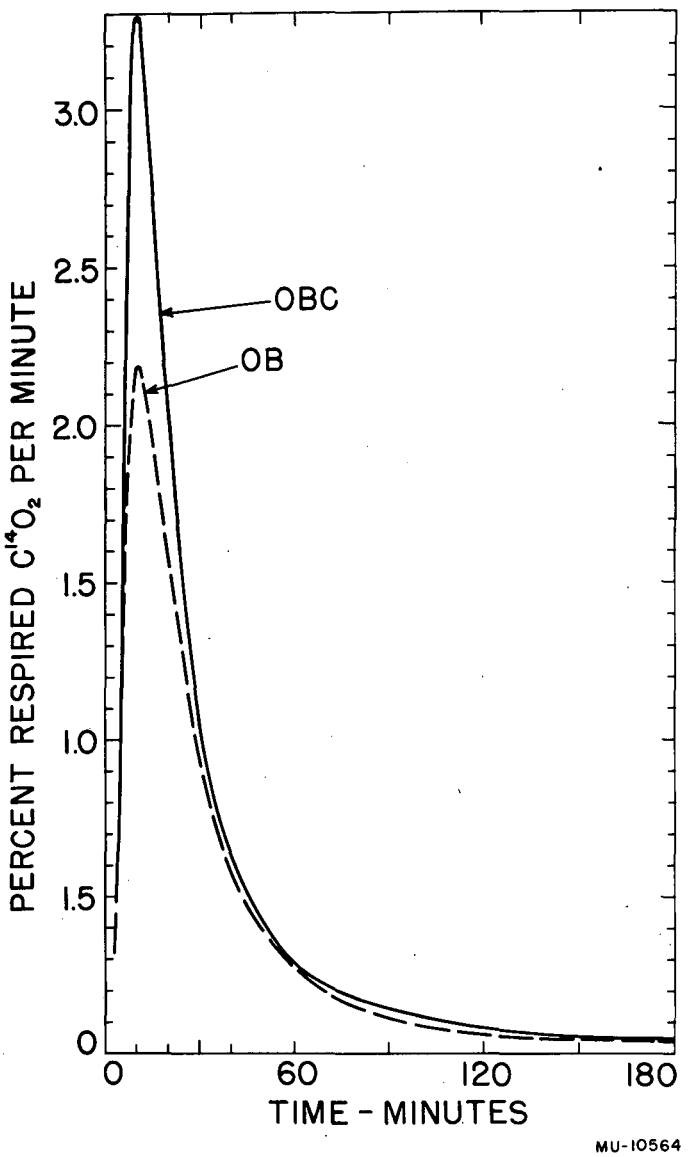

Fig. 9. Rate of excretion of sodium acetate-C^{14} injected i.p.

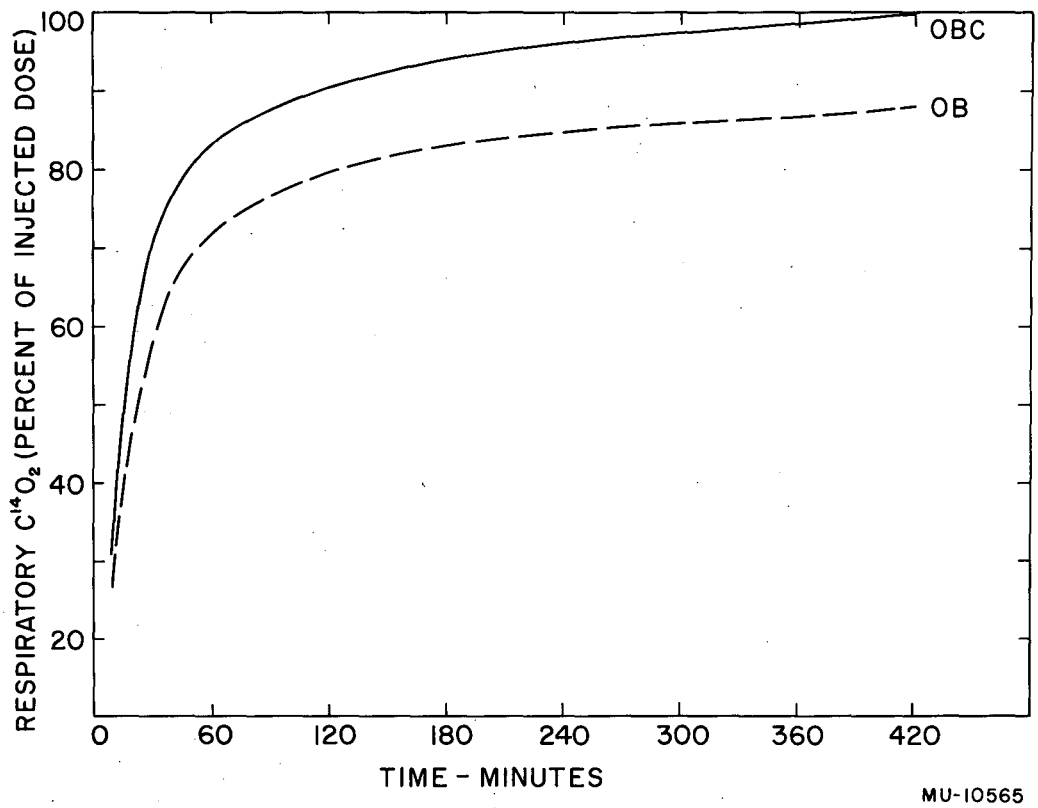

Fig. 10. Cumulative excretion of sodium acetate-C^{14} injected i.v.

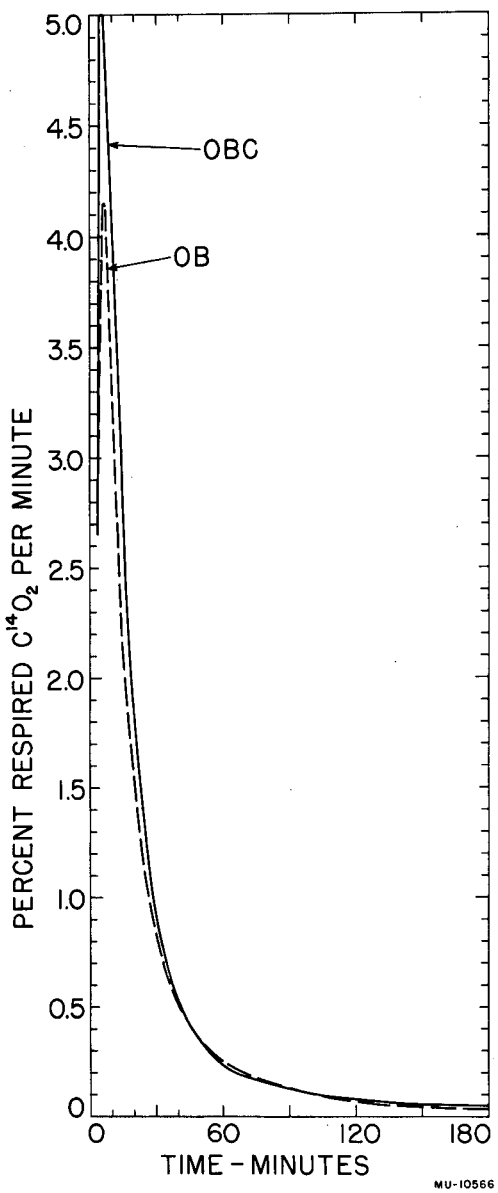

Fig. 11. Rate of excretion of sodium acetate-C^{14} injected i.v.

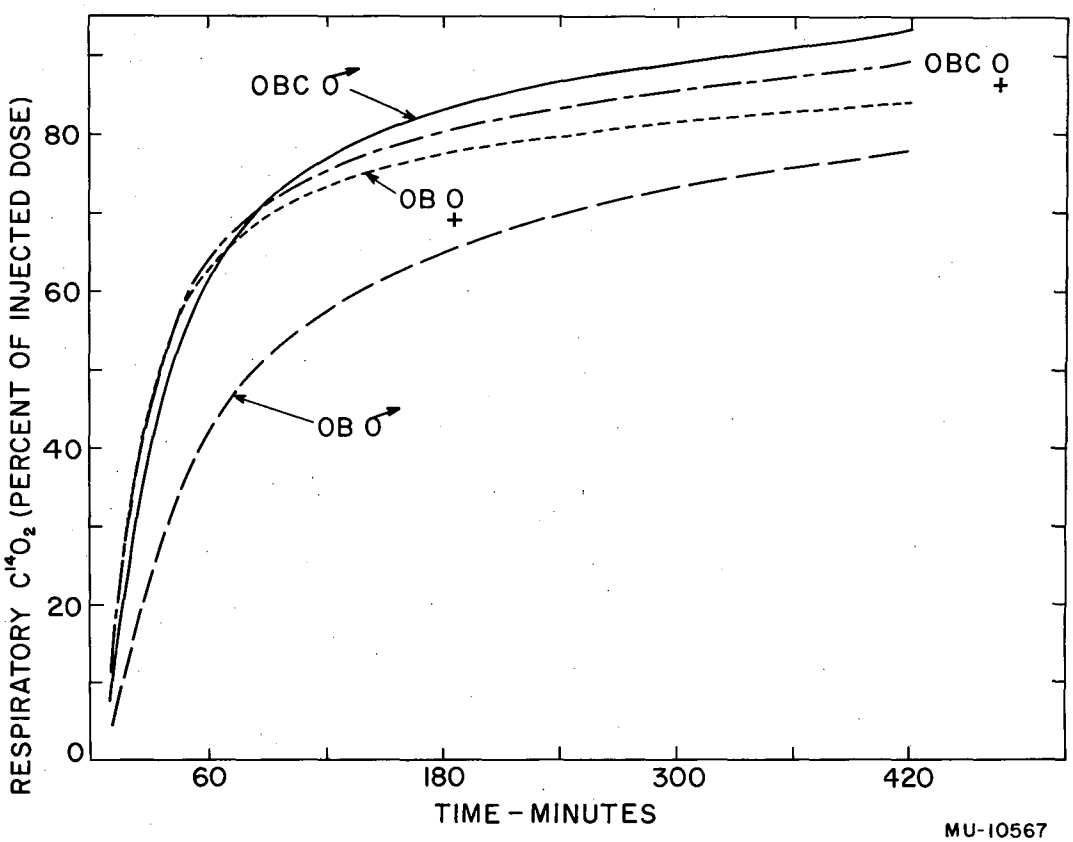

Fig. 12. Cumulative excretion of glucose-$C^{14}{}_6$ injected i.v.

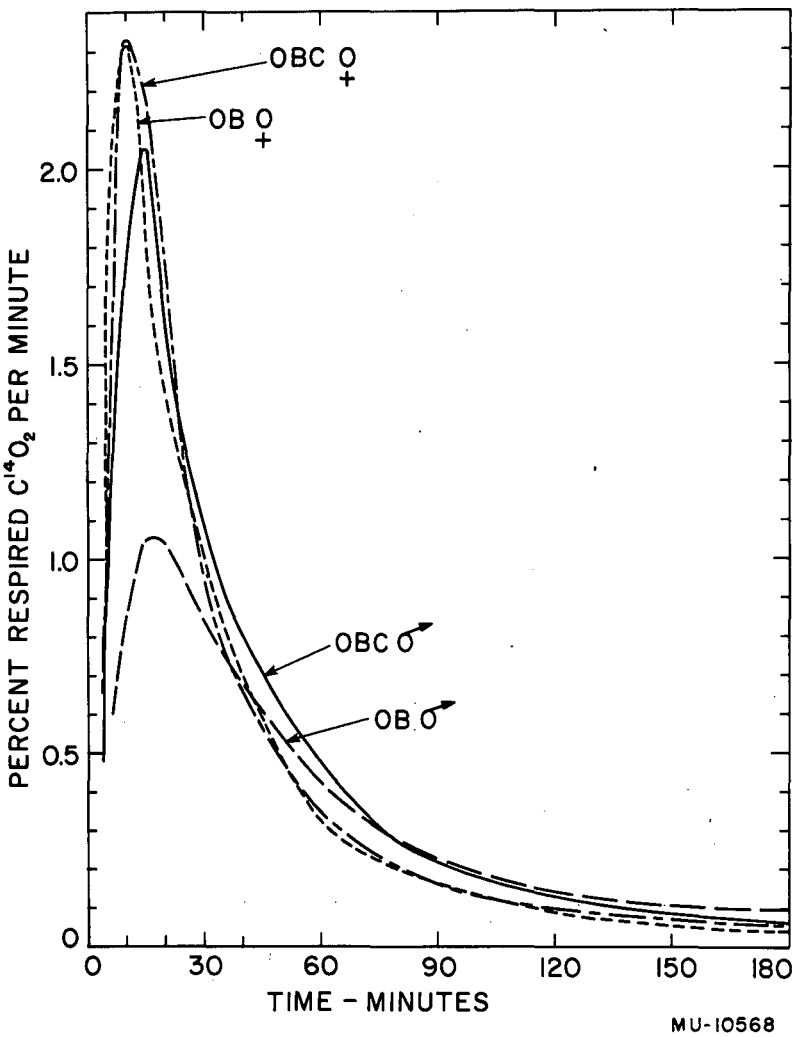

Fig. 13. Rate of excretion of glucose-C^{14}_6 injected i.v.

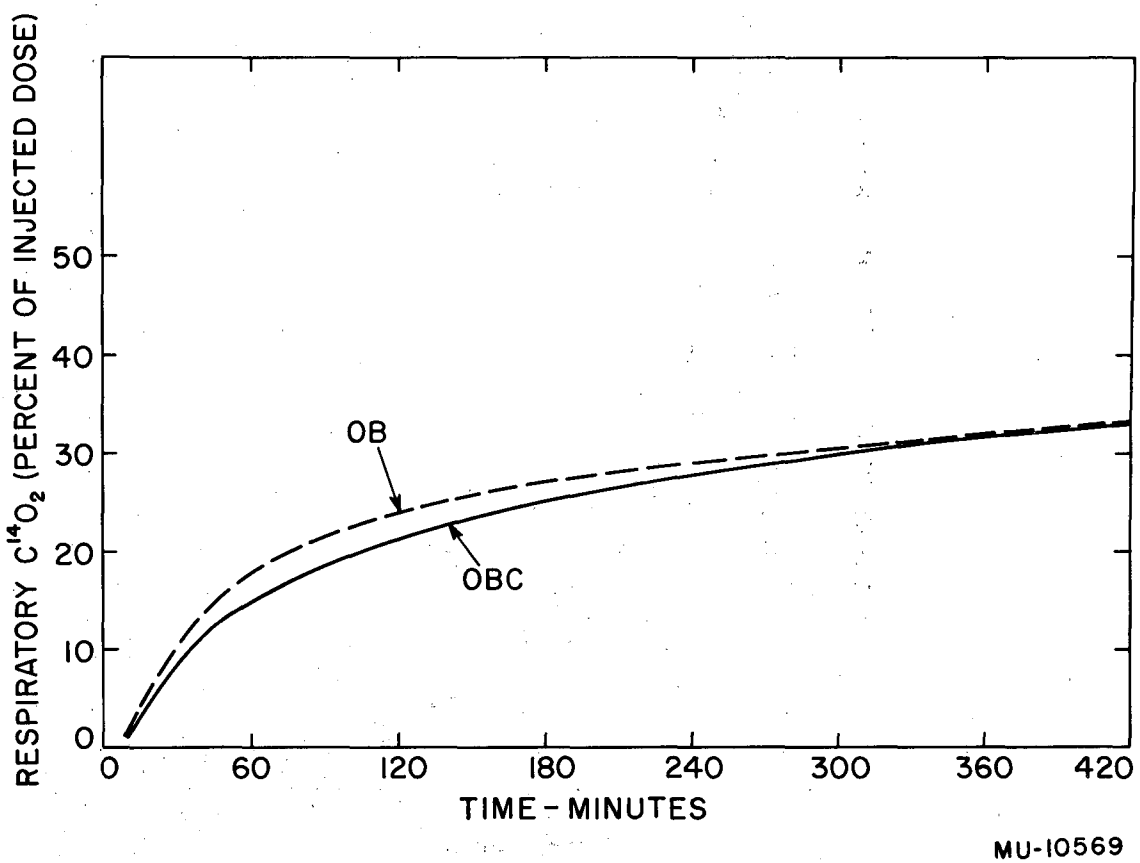

Fig. 14. Cumulative excretion of glycine-2-C^{14} injected i.p.

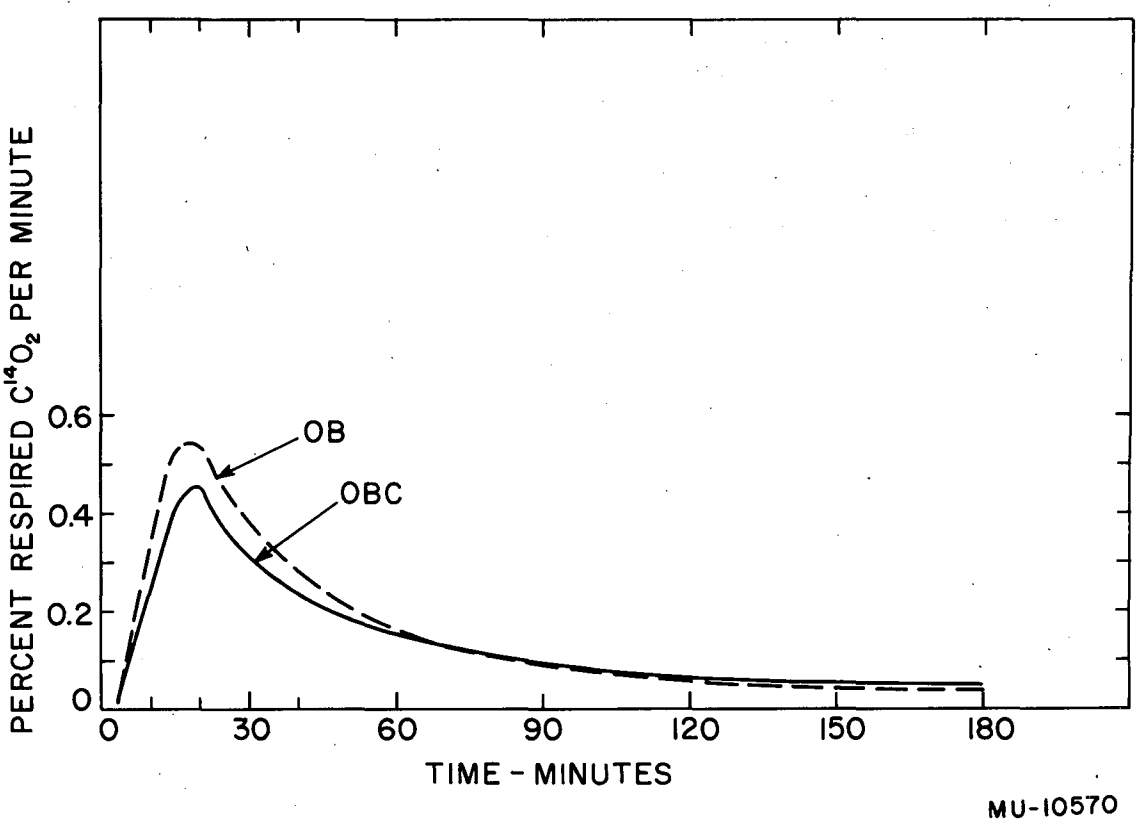

Fig. 15. Rate of excretion of glycine-2-C^{14} injected i.p.

between our and the Guggenheim-Mayer work on one hand and the Parson-Crispell work on the other hand is not evident.

In the first experiments involving the metabolism by obese mice of i.p.-injected glucose we found a rather wide variation among animals, depending to a large extent on their physical activity. In an attempt to reduce this variation, and also to eliminate the possibility of poor absorption of the i.p. glucose by the obese mice, the experiments were repeated, injecting the flucose i.v. Results are shown in Figs. 12 and 13. In these experiments a sex difference became apparent in the obese mice. It will be seen in both the curve for cumulative percent recovery of $C^{14}O_2$ (Fig. 12) and the curve for rate of recovery of $C^{14}O_2$ (Fig. 13) that the male and female controls and the female obese mice metabolize glucose in essentially the same manner, while the obese males present an entirely different picture. From the observations of earlier workers that diabetes mellitus frequently is associated with hereditary diabetes, it is quite probable that these males had a greater diabetic tendency than the females, although the gross clinical test for urine sugar was negative. Further support of this theory is found in the observation of one male mouse that gave a very positive urine-sugar test, and whose carbohydrate metabolism was impaired to such an extent that only 10% of the injected glucose was recovered as CO_2 in a 7-hour period. The administration of insulin with the glucose tripled the respiratory metabolism of the glucose. Starving the mice for 24 hours prior to the glucose experiments did not change the respiratory patterns.

As can be seen from Figs. 14 and 15, there was no difference between obese and control mice in the metabolism of glycine.

$C^{14}O_2$ EXCRETION PATTERNS AND METABOLIC ACTIVITY LEVEL IN RATS

Martha R. Kirk, B. M. Tolbert, and Samuel Lepkovsky

The level of metabolic activity in an animal system should have an effect on the breath excretion pattern of C^{14}-labeled metabolites. The present series of experiments is designed to determine and to measure this effect.

Experimental

By a long training period rats may be taught to consume their total food intake for 24 hours in 2 hours. On such a schedule they grow and develop normally. We have used such trained rats to study respiratory carbon-14 patterns as a function of time after feeding. In order to measure differences at these various metabolic levels, 2-hour excretion patterns were determined for rats injected with a C^{14}-metabolite at 1 hour, 8.5 hours, and 22 hours after the end of the feeding period. Metabolites used in this way were acetate-2-C^{14}, glucose-$C^{14}{}_6$, fructose-$C^{14}{}_6$, and glycine-2-C^{14}. These were administered intraperitoneally in 2-mg quantities in 0.2 ml water, and contained approximately 20 μc C^{14}. Respiratory patterns were measured for at least 4 rats (2 males and 2 females) at each interval after feeding. At the end of the respiratory measurement the animals were sacrificed and further analyses are being made by Dr. Lepkovsky and his group in the Poultry Husbandry Department.

Results

Average cumulative excretion in percent of C^{14} injected is shown for acetate-2-C^{14}, glucose-$C^{14}{}_6$, fructose-$C^{14}{}_6$, and glycine-2-C^{14} in Table III and also in the graphs (Figs. 16 and 17). Also in Table III is the average excretion of CO_2 in milligrams per minute corrected to a normal animal weight of 250 g by the ratio

$$\left(\frac{250}{W}\right)^{3/4}$$

where W is the animal's weight in grams.[1] Figures 18, 19, 20, and 21 show the specific activity (C^{14}/CO_2) patterns in millimicrocuries per gram carbon standardized to 20 microcuries injected dose and 250 grams rat weight

$$\left(\frac{W}{250}\right)^{3/4}.$$

[1] M. Kleiber, Hilgardia 6, 315 (1932); Physio Rev. 27, 511 (1947).

Table III

Cumulative excretion of $C^{14}O_2$ from rats at various times after feeding

Metabolite	Time of injection (hours after feeding)	Cumulative $C^{14}O_2$ excretion (% of injected C^{14}) Minutes after injection 0-20	40	60	90	120	Average mg CO_2/min
Acetate-2-C^{14}	1	9.71	22.48	30.95	39.60	44.23	7.52
	10.5	9.37	22.87	33.14	42.76	48.46	8.42
	22	10.44	24.63	34.08	44.27	49.68	7.59
Glucose-C^{14}_6	1	2.95	9.36	16.81	25.69	30.65	9.07
	10.5	3.46	10.60	17.90	26.41	32.34	8.55
	22	1.31	5.35	9.91	17.60	23.30	6.36
Fructose-C^{14}_6	1	3.95	11.20	17.21	23.59	27.78	8.88
	10.5	2.61	8.68	14.57	21.84	27.85	8.39
	22	1.71	5.95	10.55	16.59	21.97	6.37
Glycine-2-C^{14}	1	2.27	5.35	7.79	9.87	11.23	10.40
	10.5	0.83	2.59	3.91	5.85	7.10	8.22
	22	0.33	1.15	1.90	3.10	4.12	7.73

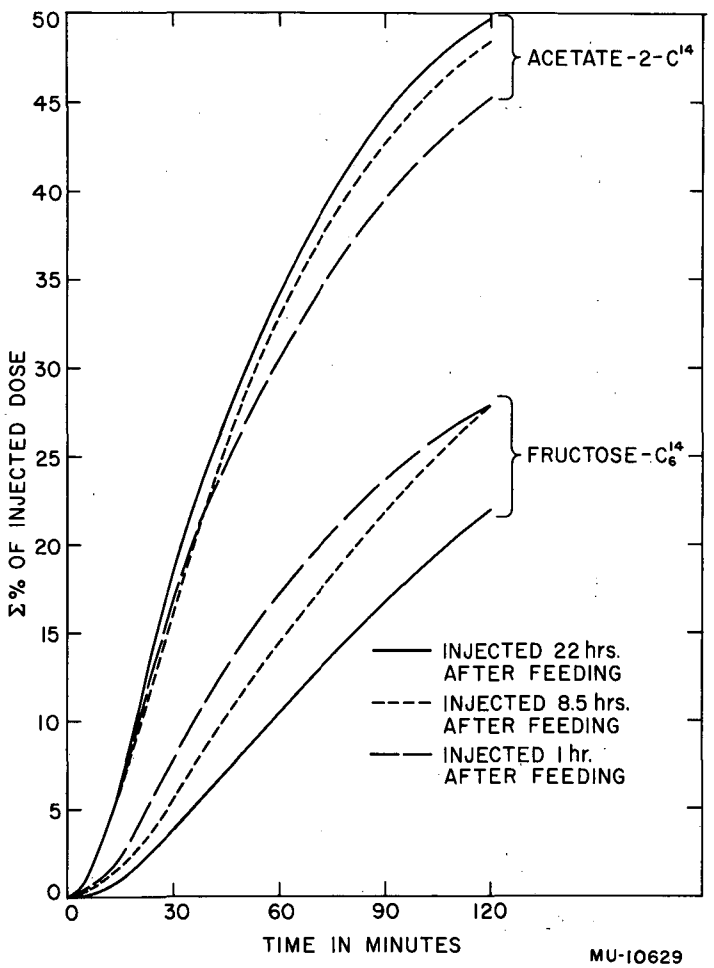

Fig. 16. Cumulative excretion of $C^{14}O_2$ from rats injected with C^{14}-labeled metabolites.

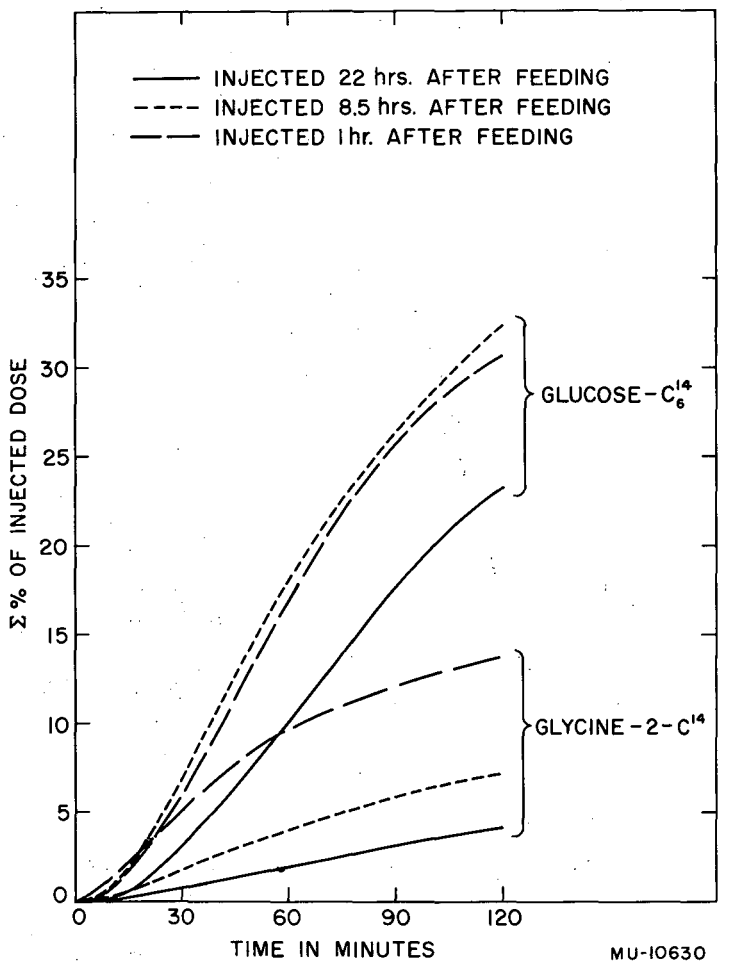

Fig. 17. Cumulative excretion of $C^{14}O_2$ from rats injected with C^{14}-labeled metabolites.

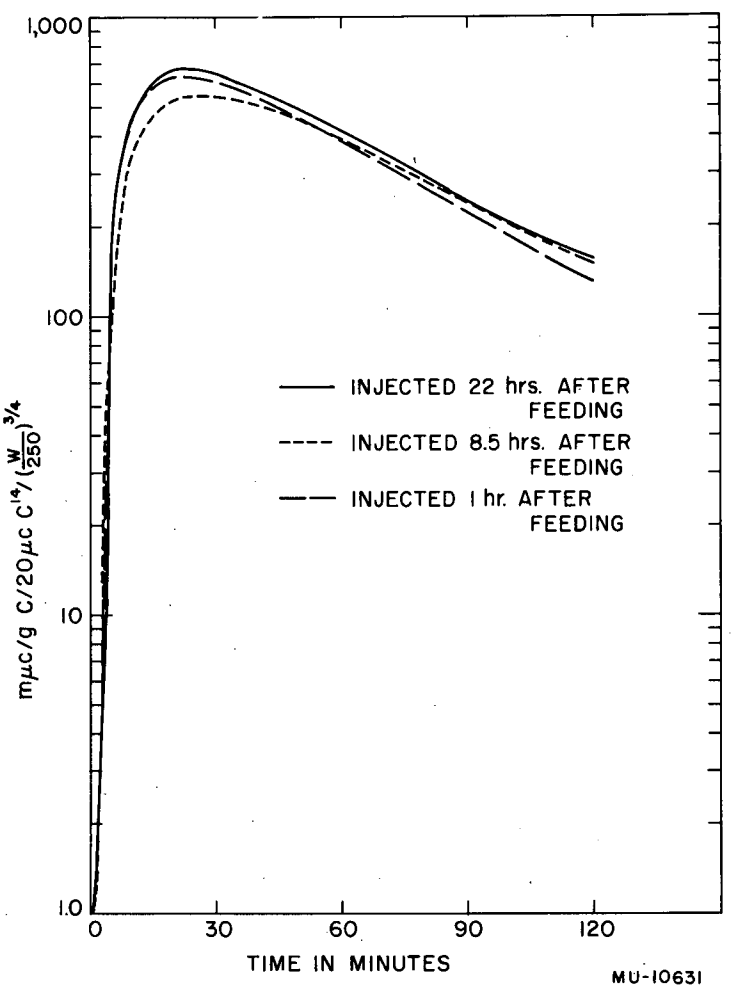

Fig. 18. Specific activity of $C^{14}O_2$ from rats injected with acetate-2-C^{14}.

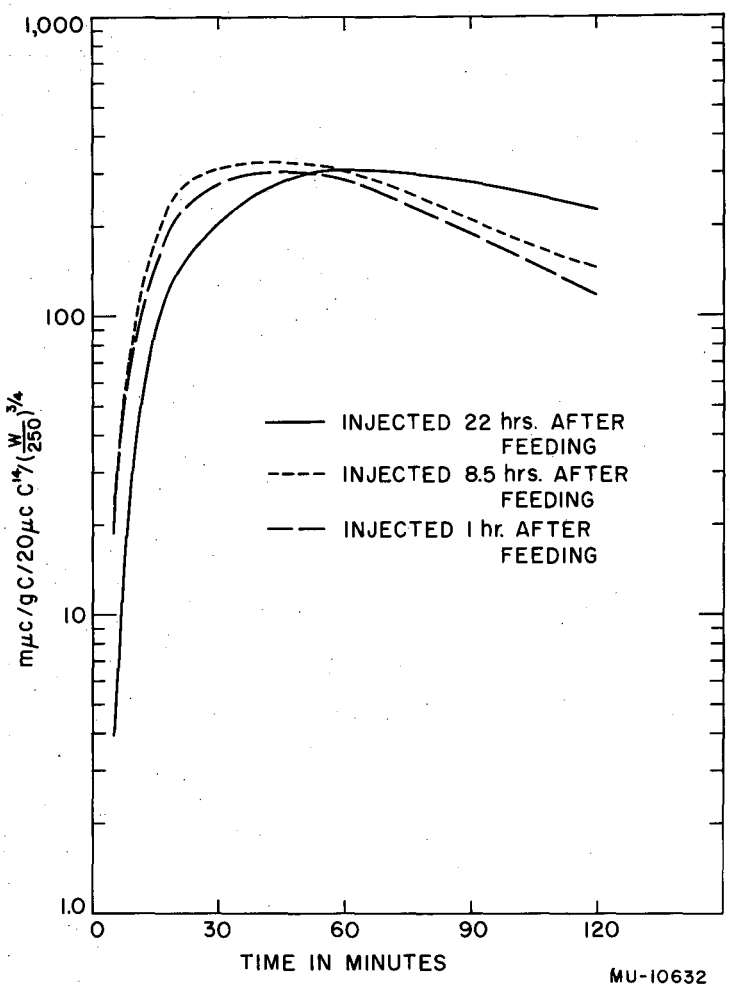

Fig. 19. Specific activity of $C^{14}O_2$ from rats injected with glucose-$C^{14}{}_6$.

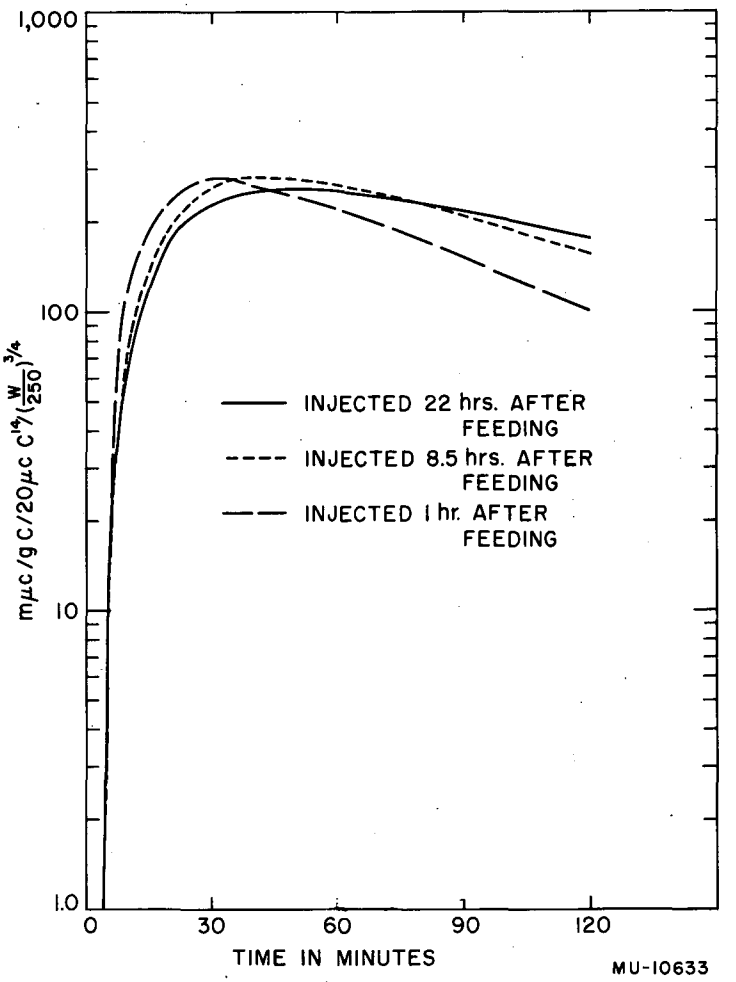

Fig. 20. Specific activity of $C^{14}O_2$ from rats injected with fructose-$C^{14}{}_6$.

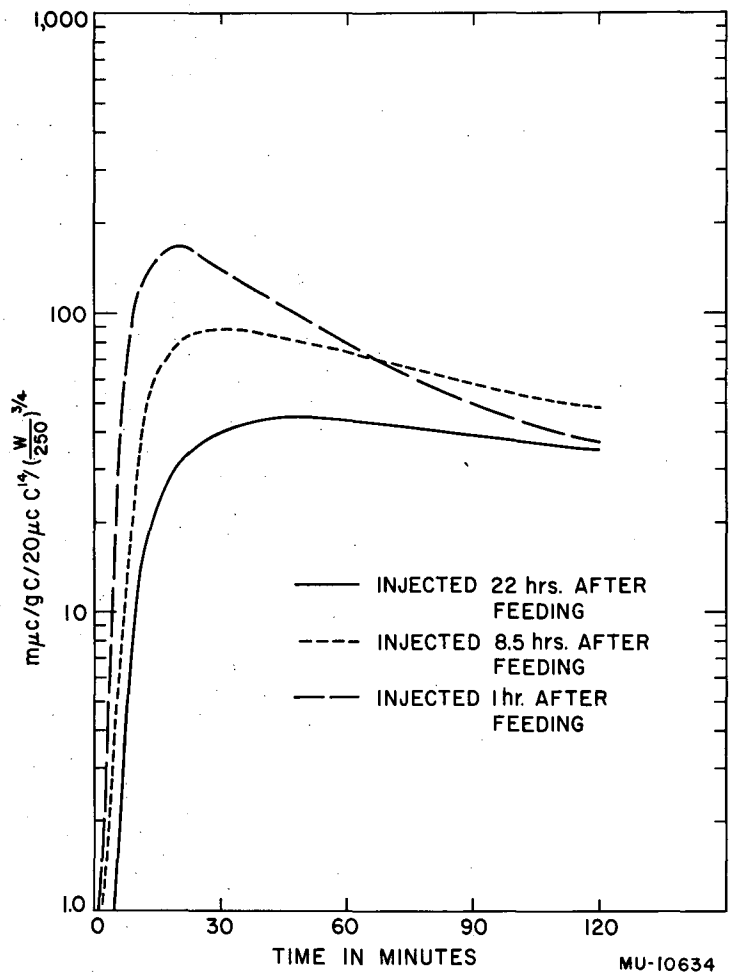

Fig. 21. Specific activity of $C^{14}O_2$ from rats injected with glycine-2-C^{14}.

Discussion

There is no significant difference in acetate oxidation as a function of time after feeding. However, glucose-$C^{14}{}_6$, fructose-$C^{14}{}_6$, and glycine-2-C^{14} are characterized by the more rapid oxidation of the metabolite by the animals injected one hour after feeding. This is shown in both the cumulative and specific activity-excretion patterns. In the case of glucose-$C^{14}{}_6$ there seems to be no real difference between the one-hour and the 8.5-hour animals; however, the one-hour animals start the oxidation of fructose-$C^{14}{}_6$ at a more rapid rate than the 8.5-hour animals. This "speeding up" of the oxidation process is particularly significant when glycine-2-C^{14} is the metabolite. Another indication of their speeded-up metabolic state is the more rapid rise in specific activity by the recently fed animals followed by a more rapid fall, after the peak excretion rate is reached.

The amount of CO_2 produced is also definitely greater shortly after feeding, indicating a higher level of metabolic activity. This is in accord with our previous observations[2] and the usual observations in basal metabolism studies. There was no observable sex difference.

[2] Martha R. Kirk, Denham Harmon, and B. M. Tolbert, UCRL-2932, March 30, 1955, p. 12.

THE INCORPORATION OF ADENINE-2-C^{14}, ADENINE-8-C^{14}, AND ADENINE-4,6-C^{14} INTO NUCLEOTIDES AND NUCLEIC ACIDS IN C_{57} MICE

Edward L. Bennett

Previous studies of adenine incorporation in this laboratory have used adenine-4,6-C^{14}, whereas adenine-8-C^{14} or adenine-1,3-N^{15} has generally been used in other laboratories. Our present knowledge of the biosynthesis of the purine ring suggests that the C-2 carbon of the purine ring may be labile and able to equilibrate with an "active formate" of the biological system. In addition, a lability of the C-8 of the purine ring is also possible but probably less likely. The exchange of formate with C-2 of inosinic acid has been demonstrated in pigeon liver homogenates,[1] and the effect of folic acid or citrovorum factor has been shown.

With one exception, experiments to date have indicated no large lability of position 8 of the purine ring in rats.[2] The one exception is a report by M. Gordon,[3] published after this research was initiated, which indicated in feeding experiments with rats that a sevenfold difference existed between the utilization of adenine-8-C^{14} and adenine-1,3-N^{15}. It should be noted that the data used were obtained by separate workers in two different laboratories.

In our experiments, mice were administered 1.2 mg of adenine-2-C^{14}, adenine-4,6-C^{14}, or adenine-8-C^{14}(20,000 dis/min/μg), and sacrificed 1 to 28 days later. Two mice were injected with folic acid antagonists, one with 1.0 mg of aminopterin (Lederle) and the other with 4.5 mg of A-methopterin (Lederle) 30 minutes prior to injection of adenine-2-C^{14}. The soluble nucleotide adenine, RNA adenine and guanine, and DNA adenine and guanine were isolated from the small intestine, large intestine, liver, carcass, and kidney, and the specific activities were determined as previously described. In addition, excretion of $C^{14}O_2$ after administration of these compounds was determined by Martha Kirk. In all cases $C^{14}O_2$ was obtained, indicating degradation of the purine ring to compounds other than allantoin. The shape of the respiratory $C^{14}O_2$ curve was different for each of the labeled adenines. These results have been discussed more fully in a previous quarterly report.[4]

---

1 J. M. Buchanan and M. P. Schulman, J. Biol. Chem. 202, 241 (1953).

2 See review by G. B. Brown and P. M. Roll, The Nucleic Acids, Ed. E. Chargaff and J. N. Davidson, Vol. II, Academic Press, New York, 1955, p. 341.

3 M. Gordon, Experientia XI, 183 (1955).

4 Edward L. Bennett, Barbara Krueckel, and Martha R. Kirk, UCRL-2932, March 30, 1955, p. 18.

In this experiment* it was desired to test the possible lability of the C-2 and (or) C-8 position of adenine. It was considered that either these positions might be labile before the adenine had been incorporated into nucleotides or nucleic acid, or the postulated exchange might occur even after the adenine had been incorporated into nucleotides and (or) nucleic acids. If the exchange occurred before adenine incorporation into nucleotides (i.e., within the first 2 hours), animals injected with adenine-2-C^{14} (or perhaps adenine-8-C^{14}) should show less adenine incorporation into nucleotides and (or) nucleic acids at short periods after administration. For this comparison, mice were sacrificed 24 hours after administration of the adenine.

We expected that if exchange of the C-2 or C-8 positions of the purine ring occurred after adenine had been incorporated into nucleotides or into nucleic acids, this would be most evident at longer time intervals after the initial incorporation of the adenine. Therefore animals were compared from 7 to 28 days after injection of the isomerically labeled adenine-C^{14}. The results of this experiment are presented in Table IV. Data are presented for the specific activity of the nucleotide adenylic acid, RNA adenine and guanine, and DNA adenine and guanine for 5 tissues of male C_{57} mice injected with 1.2 mg of adenine-2-C^{14}, adenine-4,6-C^{14}, and adenine-8-C^{14} and sacrificed at intervals ranging from 1 to 28 days later. It must be remembered, in comparing the specific activities of the tissues, that this is a single experiment and represents comparisons between single animals. It is clear, however, that no large difference such as was reported by Gordon for adenine-8-C^{14} and adenine-1,3-N^{15} from feeding experiments in the rat exists in the mouse when adenine-4,6-C^{14} or adenine-8-C^{14} is given introperitoneally. It would appear to us unlikely that species difference can explain the results, inasmuch as Long-Evans rats injected with adenine-8-C^{14}(1.3 mg/170 g rat) had nucleotide and nucleic acid specific activities in the liver approximately twice those found for a 32-g C_{57} mouse injected with 0.12 mg of adenine. (Compare Table VI of this report with Table II of UCRL-3068, p. 15)

On the other hand, the comparisons that can be made between the specific activity of the nucleic acids after adenine-2-C^{14} and adenine-4,6-C^{14} administration would indicate that an exchange of the C-2 position may indeed occur. Although for any given tissue exceptions can be found, in general the ratio of adenine-2-C^{14}/adenine-4,6-C^{14} is less than one and appears to decrease with time. The difference does not seem to be as marked for the nucleotide fraction. Before speculating in detail on the mechanisms involved, however, we should like to repeat the experiment.

In addition, a comparison of the adenine/guanine ratio in the RNA and in the DNA of the various tissues indicates that this ratio decreases with time, suggesting an apparent more rapid renewal of the adenine than the guanine in the nucleic acids. In an examination of the acid-soluble fraction shortly after administering adenine, however, a similar decrease in the ratio of the specific activities of the acid-soluble 5'-adenylic acid

---

* The experiments reported here are preliminary experiments and the results and interpretations must be confirmed by further experiments. In addition, the RNA-adenine analyses are not yet completed.

Table IV

Specific Activity of 5-Adenylic Acid, RNA Adenine and Guanine, and DNA Adenine and Guanine in C_{57} Mice after Administration of Adenine-2-C^{14}, Adenine-4,6-C^{14} or Adenine-8-C^{14}

Time after Injection	Compound	5-Adenylic Acid s.a.	5-Adenylic Acid % Ad-4,6	RNA Adenine s.a.	RNA Adenine % Ad-4,6	RNA Guanine s.a.	RNA Guanine % Ad-4,6	Ratio Ad/Gu	DNA Adenine s.a.	DNA Adenine % Ad-4,6	DNA Guanine s.a.	DNA Guanine % Ad-4,6	Ratio Ad/Gu
						Small Intestine							
24 hours	Ad-4,6-C^{14}	1730		980		108		9.1	470		85		5.5
	Ad-8-C^{14}	1380	80	735	75	78	74	9.4	387	83	61	72	6.3
	Ad-2-C^{14}	1530	88	946	97	125	116	7.5	495	105	79	94	6.3
8 days	Ad-4,6-C^{14}	66				24.3			35		7.9		4.4
	Ad-8-C^{14}	41	62			16.4	67		26	74	6.5	82	4.0
	Ad-2-C^{14}	74	112	78		23.4	95	3.3	22	63	5.3	66	4.1
15 days	Ad-4,6-C^{14}	19.5				14.5			20		5.4		3.9
	Ad-8-C^{14}	25	128			14.0	96		22	110	7.4	137	3.0
	Ad-2-C^{14}	24	125	30		13.1	89		9.2	46	1.8	33	5.1
28 days	Ad-4,6-C^{14}	5.5	115			5.4			10.2		2.5		4.1
	Ad-8-C^{14}	6.3				6.3	126		10.7	105	4.1	165	2.6
						Large Intestine							
24 hours	Ad-4,6-C^{14}	1390		865		144		6.0	360		52		6.9
	Ad-8-C^{14}	1490	107	905	105	88	61	10.3	345	96	39	75	8.8
	Ad-2-C^{14}	1635	117	1050	121	140	97	7.5	475	132	61	117	7.8
8 days	Ad-4,6-C^{14}	103				39			53		11.5		4.6
	Ad-8-C^{14}	81	79			31	80		33	62	9.3	81	3.5
	Ad-2-C^{14}	138	134	113		42	108	2.7	66	124	14.3	124	4.6
15 days	Ad-4,6-C^{14}	33				24			19		5.4		3.5
	Ad-8-C^{14}	58	175			—			—		—		
	Ad-2-C^{14}	37	112	32		16	67	2.0	8.6	45	2.8	52	3.1
28 days	Ad-4,6-C^{14}	13.7				8.6			17		5.0		3.4
	Ad-8-C^{14}	14.9	108			12.1	140		9.9	58	2.8	56	3.5
						Liver							
24 hours	Ad-4,6-C^{14}	1670		670		67		10	—		—		—
	Ad-8-C^{14}	1397	34	432	64	50	75	8.6	11.8	—	2.5	—	4.7
	Ad-2-C^{14}	1410	85	563	84	50	75	11	16	—	2.5	—	6.4
8 days	Ad-4,6-C^{14}	258				156			33		9.7		3.4
	Ad-8-C^{14}	221	85			122	78		23	69	6.4	66	3.6
	Ad-2-C^{14}	180	70	450		89	57	5.0	11.8	36	3.0	31	3.9
15 days	Ad-4,6-C^{14}	86				114			68		18		3.7
	Ad-8-C^{14}	90	105			115	101		46	68	15	83	3.0
	Ad-2-C^{14}	70	82	215		63	55	3.4	9	13	3.0	17	3.0
28 days	Ad-4,6-C^{14}	16				36			32		13		2.5
	Ad-8-C^{14}	16	100			43	119		19	60	8.8	68	2.2

Table IV Continued

Time after Injection	Compound	5-Adenylic Acid s.a.	% Ad-4,6	RNA Adenine s.a.	% Ad-4,6	RNA Guanine s.a.	% Ad-4,6	Ratio Ad/Gu	DNA Adenine s.a.	% Ad-4,6	DNA Guanine s.a.	% Ad-4,6	Ratio Ad/Gu
						Carcass							
24 hours	Ad-4,6-C^{14}	210		253		31		8.1	182		34		5.3
	Ad-8-C^{14}	230	109	236	93	25	81	9.4	162	89	31	92	5.1
	Ad-2-C^{14}	317	150	264	104	35	113	7.6	141	77	29	85	4.9
8 days	Ad-4,6-C^{14}	167				51			33		11		3.0
	Ad-8-C^{14}	151	90			52	102		18	55	—	—	—
	Ad-2-C^{14}	190	114	168		37	72	4.5	18	55	7	64	2.6
15 days	Ad-4,6-C^{14}	167				54			15.3		5.0		3.1
	Ad-8-C^{14}	150	90			53	98		14.9	97	4.7	94	3.2
	Ad-2-C^{14}	150	90	128		39	72	3.3	5.3	35	2.0	40	2.7
28 days	Ad-4,6-C^{14}	116				45			13.9		5.5		2.5
	Ad-8-C^{14}	112	96			47	104		11.3	81	3.3	59	3.5
						Kidney							
24 hours	Ad-4,6-C^{14}	1060		475		136		3.5	9.9		< 1		>10
	Ad-8-C^{14}	1172	110	485	102	133	98	3.6	13	131	< 1		>10
	Ad-2-C^{14}	1029	97	407	86	114	84	3.6	6.6	67	< 2		> 3
8 days	Ad-4,6-C^{14}	218				200			49		14		3.5
	Ad-8-C^{14}	165	75			192	96		23	47	10	71	2.3
	Ad-2-C^{14}	175	80	285		168	84	1.7	14	28	3.8	26	3.8
15 days	Ad-4,6-C^{14}	93				157			—		—		—
	Ad-8-C^{14}	100	107			123	78		40	—	19	—	2.1
	Ad-2-C^{14}	66	71	126		92	59	1.4	13	—	4.2	—	3.1
28 days	Ad-4,6-C^{14}	28				52			48		19		2.5
	Ad-8-C^{14}	28	100			61	119		80	165	22	115	3.6

* The animals were intraperitoneally injected with 1.2 mg of adenine labeled in the indicated position and sacrificed at the appropriate time interval after injection. The specific activity of the adenine injected was 20,000 dis/min/μg. All activities have been calculated in terms of μg equivalent of adenine.

to 5'-guanylic acid has been observed. If these compounds are serving as precursors for the nucleic acid, a change in this ratio may be sufficient to explain the observed change in the nucleic acid adenine/guanine specific-activity ratio.

In a related experiment, A-methopterin and aminopterin were administered to two male C_{57} mice 30 minutes prior to injection of the adenine-2-C^{14}. It was expected that the specific activity in the nucleotides and nucleic acids might be increased in the A-methopterin- or aminopterin-treated animals as compared to the control if the 2-position of the purine ring were in equilibrium with fomate through the citrovorum factor. As shown in Table V, a changed pattern of incorporation of adenine-2-C^{14} was noted in the drug-treated animals, the effect being different in the different tissues. In addition, the effect was much larger upon the incorporation of adenine into guanine, and in most tissues a 50% to 100% increase in the specific activity of the RNA guanine was noted. An increased incorporation into DNA guanine of the large and small intestine was also observed, whereas a large inhibition was found in the DNA of the liver. However, we do not believe that this effect is due to a decreased labilization of the 2-position of the adenine, but rather to effects of the drug upon nucleic acid synthesis and perhaps particularly upon guanine synthesis. In this case, it may be suggested that the animal is much less able to make the needed guanine for the nucleic acid and so draws upon the adenine pool. Another factor may be a decreased absolute amount of nucleic acid in such animals. Similar results have been reported with adenine-1,3-N^{15} in aminopterin-treated Sherman rats.[5]

Another factor affecting the incorporation of adenine-C^{14} that has been investigated is the effect of varying the amount of adenine injected. In our standard experiments we have administered 1.2 mg of adenine to 25- to 30-g C_{57} mice. This is a relatively large amount, since little or no free adenine exists in the mouse. In Table VI are shown the results obtained when 0.12 mg (10% of the usual amount) was administered to a 32-g C_{57} mouse. The most striking effect observed at 24 hours is the greatly increased ratio of adenine/guanine specific activity obtained with the smaller dose. In addition, in the liver and kidney the specific activity of the adenylic acid nucleotides and the RNA-adenine is considerably higher than would be expected on a proportional basis for the dose given. The variation in distribution of adenine as a function of dosage probably explains the differences reported in the ratios of specific activity of liver as compared to intestine. In general, when smaller quantities of adenine have been administered, the specific activity of the liver adenine derivatives have been higher than that of the intestines, while when larger amounts of adenine have been administered, the intestines have had a higher specific activity than the liver. This emphasizes the importance of many factors, including time and dosage, in determining the distribution of adenine and probably of other precursors in nucleic acids, and the danger of drawing too many generalizations from ratios of specific activity between tissues or between adenine and guanine.

---

[5] D. A. Goldthwait and A. Bendich, J. Biol. Chem. 196, 841 (1952).

Table V

Effect of Aminopterin and A-Methopterin upon the Incorporation of Adenine-2-C^{14} into Nucleotides and Nucleic Acids of C_{57} Male Mice*

Tissue	Treatment	5-Adenylic Acid % Control	RNA Adenine % Control	RNA Guanine % Control	Ad/Gu Ratio	DNA Adenine % Control	DNA Guanine % Control	Ad/Gu Ratio
Small Intestine	Control				7.5			6.3
	Aminopterin	175	136	162	6.4	93	138	4.2
	A-Methopterin	126	101	97	7.9	73	106	4.3
Large Intestine	Control				7.5			7.8
	Aminopterin	146	131	193	5.1	83	180	3.6
	A-Methopterin	122	107	165	4.9	98	169	4.5
Liver	Control				11			6.4
	Aminopterin	66	86	138	7.1	55	65	5.6
	A-Methopterin	84	79	80	11	32	20	10
Carcass	Control				7.6			4.9
	Aminopterin	84	101	90	8.5	94	97	4.8
	A-Methopterin	97	84	78	8.0	93	89	5.1
Kidney	Control				3.6			
	Aminopterin	102	118	154	2.7	210		
	A-Methopterin	151	134	153	3.1	53		

*) 1.0 mg of aminopterin or 4.5 mg of A-methopterin was injected into the mouse 30 minutes prior to the intraperitoneal administration of 1.2 mg of adenine-2-C^{14}. The mice were sacrificed 24 hours later. To calculate specific activity refer to the 24-hour adenine-2-C^{14} data in Table IV.

ZN-1449

Table VI

Effect of Dosage upon Incorporation of Adenine-4,6-C^{14} into Nucleotides and Nucleic Acids of C_{57} Male Mice*

Tissue	Amount of Adenine-4,6-C^{14}	% of Control						
		5-Adenylic Acid	RNA Adenine	RNA Guanine	Ad/Gu Ratio	DNA Adenine	DNA Guanine	Ad/Gu Ratio
Small Intestine								
	1.2 mg				9.1			5.5
	0.12 mg	10	8.5	4.5	17	7.4	2.8	14
Large Intestine								
	1.2 mg			6.7	6.0			6.9
	0.12 mg	17	12	6.3	12	10	3.2	23
Liver								
	1.2 mg				10			—
	0.12 mg	22	16		21			>20
Carcass								
	1.2 mg				8.1			5.3
	0.12 mg	13	10	6	13	2.6	<2	>10
Kidney								
	1.2 mg				3.5			>10
	0.12 mg	21	28	16	6.0	22	--	>7

*) 1.2 mg or 0.12 mg of adenine-4,6-C^{14} was administered by intraperitoneal injection to two male C_{57} mice. They were sacrificed 24 hours later. To calculate specific activity refer to the 24-hour adenine-4,6-C^{14} data in Table IV.

NUCLEAR CHEMISTRY

Glenn T. Seaborg and Isadore Perlman in charge

OPTICAL SPECTROSCOPY

Color Centers and Luminescence in Lanthanum Chloride-Europium Chloride Crystals

John G. Conway, Ralph D. McLaughlin, and Dieter M. Gruen

The color-center formation reported in the preceding quarterly report has been extensively investigated. Single crystals of $LaCl_3$ containing 10%, 1%, and 0.01% $EuCl_2$ have been grown. The crystals exhibit the following properties:

(a) color-center formation,
(b) phosphorescence,
(c) fluorescence,
(d) thermal luminescence,
(e) dichroism.

The 0.01% $EuCl_2$-containing crystal could be bleached of the color center by intense gamma radiation.

Peaks in a glow curve have been found. When the crystal is then raised to the temperature indicated by the peak a luminescence is observed, and a change in the absorption is noted.

Low-Temperature Dewar for Zeeman Effect in Absorption

John G. Conway and Ralph D. McLaughlin

A double, stainless steel Dewar with quartz windows has been fabricated. The windows are cemented in place with Araldite. This seal has been tested three times, with liquid hydrogen used as a coolant, and has held vacuum. When liquid helium is used the seal does not hold. Because of this difficulty we are now equipping the spectroscopy room so that liquid hydrogen work can be carried on. This work should be completed in three weeks and the Zeeman studies started.

THREE-MILLIMICROSECOND METASTABLE STATE IN LEAD-209

Donald Strominger, John O. Rasmussen, and Frank S. Stephens

The fast-coincidence counting equipment described in previous reports[1] was used to investigate the possibility of the existence of metastable states in the Ac^{225} chain. The results of these experiments indicate the existence of a 3.1 ± 1.0-millimicrosecond isomer of Pb^{209}. This half life is exhibited by a 120-kev E1 gamma transition and other gamma transitions following the 120-kev gamma transition in the decay of Tl^{209} to Pb^{209}.

Upper limits for the half lives of the following gamma transitions were set: $t_{1/2}$ < three millimicroseconds for a gamma transition of approximately 100 kev following the alpha decay of Ac^{225}; $t_{1/2}$ < one millimicrosecond for a gamma transition of 220 kev following the alpha decay of Fr^{221}; and $t_{1/2}$ < 2 millimicroseconds for a 434-kev gamma transition following the beta decay of Bi^{213}.

THE CRYSTAL STRUCTURE OF AMERICIUM METAL

Peter Graf and Burris B. Cunningham

Several preparations of americium metal have been made in order to obtain metal that is well crystallized and yields x-ray diffraction patterns that may be interpreted. The americium metal is produced in a tantalum crucible by the high-vacuum reduction of AmF_3 with barium metal. After the metal is produced by the high-temperature reaction (~1200° C), it is annealed for 10 hours with the temperature slowly reduced from 800° C to room temperature. This is done in the crucible in which the reduction is carried out and without breaking the vacuum.

Production and annealing of americium metal in this fashion has yielded two pieces of metal that have given x-ray diffraction patterns. One pattern has been indexed double hexagonal close packed, giving for americium a metallic radius of 1.82 Å and a calculated metal density for this phase of 11.87 g/cm^3. This is in close agreement with the experimentally observed density of 11.88 reported by Westrum and Eyring (J. Amer. Chem. Soc. 73, 3396 (1951)).

Some difficulties have been experienced in properly aligning the cameras and x-ray beam and in properly collimating the beam; these problems are currently being solved and a high-temperature camera is being readied for use in obtaining complete x-ray information about all the phases of americium metal. It is also planned to make melting point and magnetic susceptibility measurements.

---

[1] J. O. Rasmussen, M. I. Kalkstein, and D. Strominger, Quarterly Reports, 1953-55.

THE REACTION PRODUCTS OF TANTALUM WITH 5.7-Bev PROTONS

James R. Grover and Glenn T. Seaborg

Yields for many of the radioactive nuclides that appear as products in the reaction of tantalum with 5.7-Bev protons are being measured radiochemically. The following table lists the results that have been obtained since the preceding quarterly report.

Cross sections for the formation of nuclides in the bombardment of tantalum with ~5.7-Bev protons

Nuclide	Cross section in millibarns	Type of Yield	Remarks
Te^{121}	6	C	a
Te^{121m}	$\lesssim 0.5$	I ?	a
Sn^{108}	1.2	C	b
Sr^{82}	1.8	C	b
Sr^{83}	0.9	C	b
Se^{72}	0.26	C	b
Se^{73}	0.44	C	b

(a) These yields are based on the total K x-ray count, not corrected for x-ray contributions from γ-ray conversion in the decay schemes of the nuclides involved.

(b) These nuclides were assumed to have a counting efficiency of 100% for positrons.

The symbols C and I designate cumulative and independent yields, respectively.

All these cross sections are based on a cross section of 8.3 millibarns[1] for the reaction $Al^{27}(p, 3pn)Na^{24}$ in an aluminum monitor foil, which was included in each bombardment.

[1] Rex H. Shudde, private communication.

ION-EXCHANGE EQUILIBRIUM STUDIES

Bertha Graus Odenheimer and Gregory R. Choppin

Experiments were carried out to determine the formation constants of the complexes that are formed between alpha-hydroxy-isobutyric acid and Cm^{244} by means of ion-exchange equilibrium measurements. The resin used was Dowex 50 (4%) in the ammonium form. The ionic strength was maintained at 0.5 M with ammonium perchlorate. The K_d's were determined for three different concentrations of alpha-hydroxy-isobutyric acid ranging from 0.001 M to 0.05 M at a pH of 2.6 to 2.7. The temperature was maintained constant in a water bath at 25.0° C.

Preliminary results indicated the need for further experiments with higher concentrations of the acid. These experiments are now in progress.

ELECTRON-CAPTURE DECAY OF POLONIUM-206

Allan B. Stoner

A study is being carried out on the nuclear energy levels in Bi^{206}, which are revealed in the electron capture decay of Po^{206}. The gamma spectrum has been measured on a NaI scintillation counter and the relative intensities of the gamma rays determined. The electrons from the conversion of these gamma rays have been observed in both permanent- and variable-field beta-ray spectrometers. The data have indicated the following gamma rays; 1031, 807, 511, 522, 338, 311, 286, and 60 kev. The energy uncertainties are ± 0.2% with the variable-field spectrometers for K/L ratio determination. These results are to be used ultimately for multipolarity assignments. This work with electron-electron coincidences will be used to construct an electron-capture decay scheme of Po^{206}.

FISSION-SPALLATION MECHANISMS

Fission and Spallation Reactions of Americium-241 with Low-Energy Alpha Particles

Bruce M. Foreman, Jr., Richard A. Glass, and Glenn T. Seaborg

Progress in the investigation of the fission and spallation reactions of Am^{241} induced by alpha particles is reported. Preliminary spallation cross sections are as follows:

Spallation cross sections (mb)				
E_α(Mev)	α, n + α, 2n	α, n	α, 2n	α, p2n
18.1	5	5	--	--
20.8	2*	(1)	(0.9)	--
31.0	77	(6.5)	(70)	0.07

* The indicated mimimum in the (α, n) reaction cross section at 20.8 Mev is probably due to experimental error since spallation cross sections rise with increasing energy in this barrier energy region.

Since the (α, n) and (α, 2n) products have approximately the same half lives, the sum of the (α, n) and (α, 2n) cross sections is measured experimentally. The partition between the reactions was estimated at 20.8 and 31.0 Mev by the following formula given by Blatt and Weiskopf (Theoretical Nuclear Physics, John Wiley and Sons, 1952):

$$\sigma(\alpha, 2n) = [\sigma(\alpha, n) + \sigma(\alpha, 2n)] \; [1 - (1 + \frac{\epsilon_c}{\theta} e^{-\frac{\epsilon_c}{\theta}}],$$

where ϵ_c = excess energy over the threshold for the (α, 2n) reaction,

θ = nuclear temperature (estimated by analogy with Pu^{239}).

The fission results are as follows:

Fission cross sections (mb)		
Nuclide	18.1 Mev	31.0 Mev
Sr^{89}	-------	13.56
Sr^{91}	0.61	17.75
$Cd^{115}+Cd^{115m}$	0.37	67.92
Ba^{140}	0.75	19.07
σ_f (total from integrated yield curves)	20.6	677

These results indicate that the Cd cross section is lower than the cross sections for Ba and Sr at 18.1 Mev and higher at 31.0 Mev. If this apparent trend is real, fission is rapidly becoming symmetric with increasing energy. The Cd cross section at 31.0 Mev, however, is subject to doubt since the integrated cross section using the value 67.92 mb is quite high. For this reason a flat fission-yield curve has been assumed for 31.0 Mev and the 677-mb cross section determined on this basis.

Fission and Spallation Reactions of Uranium-235 with Low-Energy Alpha Particles

Robert Vandenbosch, Richard A. Glass, and Glenn T. Seaborg

Cross sections for the (α, fission), (α, xn), and (α, pxn) reactions of U^{235} are being measured. Preliminary results for some of the spallation reactions are listed below.

	U^{235} cross sections (mb)		
E(Mev)	(α, 3n)	(α, p)	$(\alpha, p2n)_{\pm}$
19		$< 10^{-4}$	--
22		.019	--
25		.1	.012
28		1.52	2.5
31	5	1.7	4
34	10	1.92	6.6
37	5	1.75	11.9

Recent emphasis has been on determining the change in the shape of the fission-yield curve as a function of helium ion energy. No results are available yet on this part of the program.

Fission and Spallation Reactions of Protactinium-231 with Low-Energy Alpha Particles

William M. Wade, Walter M. Gibson, Richard A. Glass, and Glenn T. Seaborg

A fission-spallation study of Pa^{231} has been under investigation for several months. During this period, a 3-mg stock of Pa^{231} has been purified, the electroplating process for target preparation worked out, and four bombardments completed. The electroplating process is of note in that 80% to 90% yields of adherent protactinium oxide have been obtained on gold target plates from a 0.1 M Na_2SO_4 solution (with flouride ion added to complex protactinium) at 5.5 volts and 300 milliamperes/cm^2. The radiochemical steps for isolation of fission and spallation products from the entire dissolved targets include a zirconium phosphate precipitation to remove zirconium and neptunium (IV) and anion-exchange column runs to separate protactinium and uranium. All operations are carried out in highly acid media to prevent hydrolysis of protactinium. Cross sections will be presented in a subsequent report.

Tritium Production in Heavy-Element Cyclotron Targets

William H. Wade, Jose Gonzalez-Vidal, Richard A. Glass and Glenn T. Seaborg

A program is under way to measure absolute tritium-production cross sections in an effort to explain the large (α, p2n) product cross sections found for many heavy-element target nuclei. The targets initially will be U^{238} and U^{235} foils.

RADIATION CHEMISTRY

Amos S. Newton, Aldo F. Sciamanna, Peter O. Strom, Jr.
Jean H. Futrell, and Sylvia S. Waters

Several investigations are under way and considerable information on the radiolysis products of several compounds has been collected, but a detailed interpretation of the mechanisms involved has not yet been worked out.

Trichlorethylene

This compound was bombarded with helium ions because it is one of several unsaturated compounds that do not polymerize. The products are shown in Table I. In bombardment No. III, 40 mole % carbon tetrachloride was added to increase the radical density to determine whether or not this would influence the degree of polymerization. The trichlorethylene used contained a trace of hydrocarbon impurity (< 1%), probably an octene, which was not separated by distillation. This accounts for the small amount of methane produced.

Table I

Products from the helium-ion irradiation of trichloethylene

Run No.	I	II	III (40% CCl_4 added)
Energy Input (ev/ml)	0.81×10^{21}	1.14×10^{21}	0.72×10^{21}
Product	Yield G (molecules/100 ev)		
H_2	0.0053	0.0061	0.0014
CH_4	0.0014	0.0015	0.0013
CO	0.0001	0.0001	0.0003
C_2H_2	trace	0.009	0.002
HCl	~ 0.62	~ 0.80	~0.91
$HC{\equiv}CCl$	~ 1.81	~ 1.59	~ 0.56
HCl + $HC{\equiv}CCl$	~ 2.43	~ 2.39	~ 1.47
$Cl{-}C{\equiv}C{-}Cl$	0.59	0.65	0.16
$CHCl_3$	trace	0.02	0.06
Polymer	~10.1	~11.7	~11.4

The principal products are monochloroacetylene, dichloroacetylene, hydrochloric acid, and "polymer." Little is known about the composition of the polymer except that it has an average molecular weight of about 380 (Rost method), a density of $d_4^{25} = 1.68$, and an index of refraction $n_D^{25} = 1.5555$. By infrared analysis, it was shown to contain some trichlorethylene and almost no hexachlorobutadiene. The lack of appreciable yield of hexachlorobutadiene is surprising and makes the mechanism difficult to formulate.

There is some question about the relative amounts of hydrochloric acid and monochloroacetylene because of the peculiar behavior of this latter compound in the mass spectrometer. A sample of the chloroacetylene from which hydrochloric acid had been separated by pumping at -160° C still shows a large mass-36 peak in the spectrum. If the sample is allowed to stand, the height of the mass-36 peak decreases. Some data on this are shown in Table II.

Table II

Mass spectrum of HC≡C-Cl observed after various treatments

m/e	Initial spectrum after HCl separation	Spectrum after standing overnight	Spectrum after liquifying at -80° C	Spectrum after freezing at -190° C	Spectrum after standing overnight	Spectrum after standing two weeks
12	4.81	4.91	4.91	4.93	4.91	5.36
24	6.11	6.13	6.15	6.14	6.11	7.59
25	12.02	17.04	13.09	17.09	16.99	17.53
35	9.44	8.32	9.51	17.44	8.33	4.87
36	26.92	21.30	27.05	66.81	21.39	2.44
37	3.11	2.70	3.08	5.70	2.69	1.53
38	8.69	6.92	8.79	21.51	6.94	0.79
47	4.76	4.87	4.86	4.89	4.86	5.13
59	11.64	11.68	11.72	11.73	11.66	11.82
60	100	100	100	100	100	100
94 (Cl-C≡C-Cl imp.)	0.53	0.61	0.56	0.64	0.61	0.61

(Some peaks -- e.g., 48, 49, 50, 61, and 62-omitted)

Since nothing was taken out of the flask except trace samples for mass spectrometer analysis, it is apparent there is a real change occurring in the compound, especially in regard to the peaks due to HCl^+ and its fragmentation products (masses 35 to 38). Since reversible reaction of this type $HC{\equiv}CCl \rightleftarrows C_2 + HCl$, is thermodynamically impossible, the change must be one in the structure of the molecule itself. This is now being investigated by infrared absorption.

Seaborg, Perlman

ALPHA-PARTICLE SPECTROSCOPY

Richard C. Pilger, Jr. and Isadore Perlman

A number of alpha-particle spectra of Th^{227} have been obtained with the 60° sector magnetic spectrograph. A tentative list of the alpha-group energies expressed as the difference in decay energy from that of the ground-state transition (6.030 Mev) and the alpha abundances, together with the values previously reported by Rosenblum,[1] follows:

	Energy Levels of Daughter (Ra^{223})			
			Alpha Abundance (%)	
	This Work	Rosenblum	This Work	Rosenblum
1.	0	0	24	19
2.	30	29	4	4
3.	61	59	25	21
4.	80	79	3	13
5.	126	110	1	2
6.	175	173	3	4
7.	235	238	1	2
8.	243		0.1	
9.	287	286	23	17
	Not observed	307	Less than 0.05	1
10.	331	332	9	15
11.	339		5	
12.	378	386	2	2

The resolution of the spectra is about 0.1%, representing a peak width at half maximum of approximately 7 kev. A representative spectrum is shown in the accompanying Fig. 1.

[1] Rosenblum, Perey, Valadares, and Guillot. Private communication reported in Hollander, Perlman, and Seaborg, Table of Isotopes, Revs. Modern Phys. 25, 469-651 (1953).

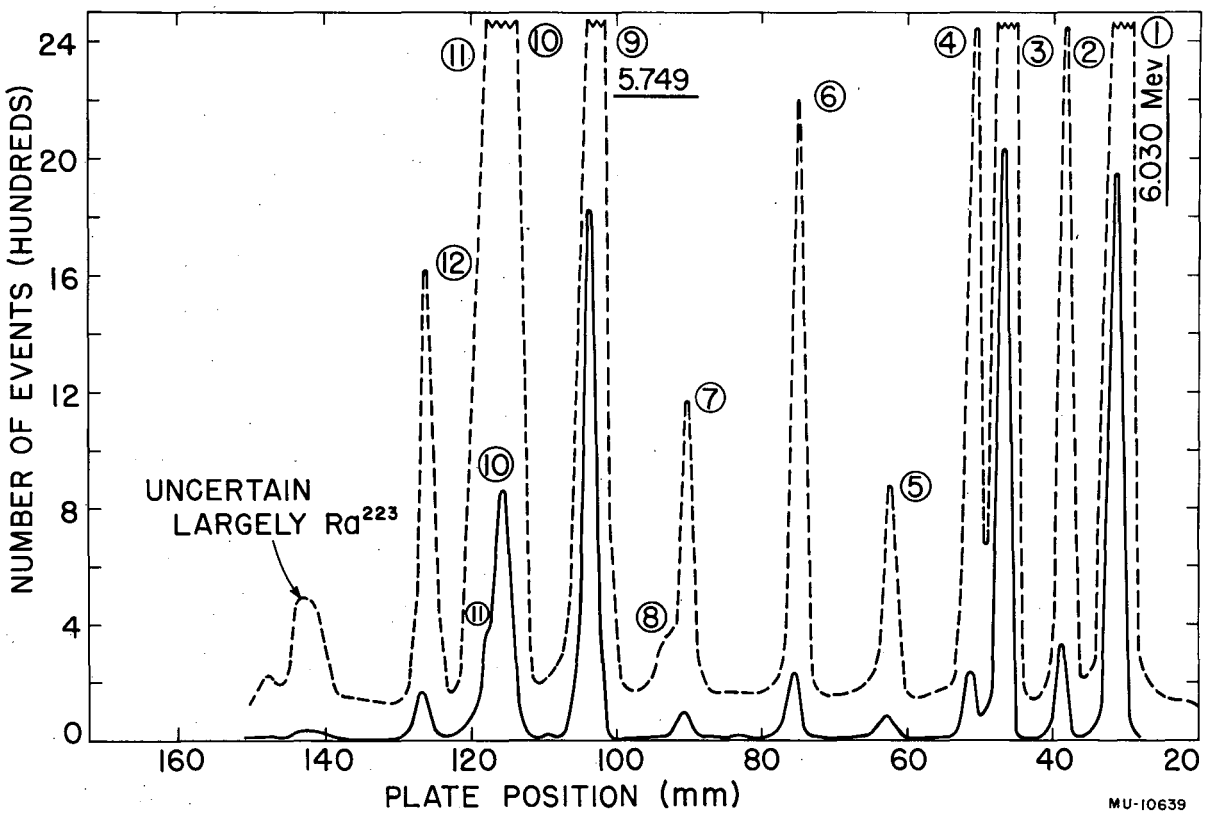

Fig. 1. Alpha-particle spectrum of Thorium-227. Energies based on the value of 6.030 Mev for the highest-energy group as determined by Rosenblum. Energy differences accurate to approximately ± 2 kev.

ELECTRON SPECTROSCOPY

Richard C. Pilger, Jr. and Isadore Perlman

The electron spectrum of Th^{227} has been investigated with two of the permanent-magnet spectrographs and with the double-focusing electromagnetic spectrograph. The spectrum of Ra^{223} has also been investigated with the latter machine.

The data have not as yet been completely evaluated. Transitions, however, have been tentatively identified in the Th^{227} decay which fit readily the energy levels known from the alpha spectra.

A pair of transitions of 234.9 and 236.8 kev, respectively, is identified by K and L_{II} conversion lines, and the transitions are considered to be E2. The L_{III} lines were not observed. The E2 assignment is partially supported by a maximum K-conversion coefficient that was determined to be 0.1 electron per photon for the approximately 237-kev gamma ray observed in coincidence with the 50-kev radiation. (See Quarterly Report, UCRL-3157, September 1955.) This assignment is at variance with that of Frilley, Rosenblum, et al.,[1] who give M1 for both transitions. Appreciable contribution of magnetic radiation would lead to a higher K-conversion coefficient than that measured by our group. It further appears that the energies of the L-conversion lines determined by these workers were somewhat low, leading to their assignment as L_I lines.

---

[1] Frilley, Rosenblum, Valadares, and Bouissieres, J. Phys. Radium 16, 378 (1955).

THE INTERACTION OF HIGH-ENERGY PROTONS WITH NUCLEI: AN INTERPRETATION OF RADIOCHEMICAL RESULTS

Lester Winsberg

In recent years data have been accumulated on the interaction of protons of energy up to 6 Bev with various target elements. Since a great effort is being expended in this field, it is appropriate to consider the significance of the results thus far obtained. We can, thereby, hope to gain insight into what is taking place inside the nucleus and also plan future experiments better.

The data on aluminum and copper are perhaps most useful since cross sections for the formation of various product nuclides have been determined over the whole range of proton energies available from accelerators.

The work of the cosmotron group on aluminum has been extended to 5.7 Bev by Benioff and Kalkstein at the Bevatron.[1,2] It is striking that the values of the cross sections to form carbon-11, nitrogen-13, oxygen-15, fluorine-18, sodium-22, and sodium-24 hardly change from 0.4 to 5.7 Bev. For beryllium-7, there is relatively little change from 1.0 to 5.7 Bev; the cross section at 0.34 Bev is much smaller. No information is available between 0.34 and 1.0 Bev to indicate at what energy the cross section for the formation of beryllium-7 rises.

The cross section for the $C^{12}(p, pn)C^{11}$ reaction also changes little from 0.4 to 5.7 Bev.[2,3]

The information on copper is somewhat confused, because the formation cross sections of the product nuclides were determined by several groups in the U.S. and Russia, each working at a different energy.[4-9]

---

1 Friedlander, Hudis, and Wolfgang, Phys. Rev. 99, 263 (1955).

2 P. Benioff and M. Kalkstein, UCRL-3068, July 6, 1955.

3 R. L. Wolfgang and G. Friedlander, Phys. Rev. 96, 190 (1954).

4 G. H. Coleman and H. A. Tewes, Phys. Rev. 99, 288 (1955).

5 Batzel, Miller, and Seaborg, Phys. Rev. 84, 671 (1951).

6 Vinogradov, Alimarin, Baranov, Lavrukhina, Baranova, and Pavlotskaya, Meeting of the Russian Academy of Science on the Peaceful Utilization of Atomic Energy, Chemistry Section, Moscow p. 132 (June 1955).

7 Murin, Preobrazhensky, Yutlandov, and Yakimov, op. cit. p. 160.

8 Friedlander, Miller, Wolfgang, Hudis, and Baker, Phys. Rev. 94, 727 (1954).

9 D. W. Barr and E. K. Hyde, UCRL-3157, September 30, 1955.

Furthermore, little is known here of the radiochemical techniques used by the Russians. Without any attempt at refinement, the values of the cross sections obtained by the various groups are plotted in Fig. 2 as a function of the proton energy. The most complete sets of cross-section values are plotted in Fig. 2a, those less complete in Fig. 2b. Cross sections that were determined at fewer than four energies are omitted. Dotted lines serve to connect points for a given nuclide but do not indicate the nature of the curve in that energy region. Solid lines are drawn where it is felt that the interpolation has some validity.

As with aluminum, there is little difference in the cross sections at 2.2 and 5.7 Bev. In the region of 480 Mev the picture is quite different. At this energy there are sharp peaks in the cross-section curves of many nuclides. However, for manganese-52, for which an excitation function has also been determined by the Brookhaven group, there appears to be disagreement with the peaked curve in Fig. 2a. They report that "the manganese-52 cross section is practically constant over the entire energy range ... from about 0.5 to 3.0 Bev."[10] There is better agreement for sodium-24. Less complete cross-section values for the formation of the lighter nuclides suggests the possible presence of a dip in the excitation functions to compensate for the peaks observed in Fig. 2. It does appear, however, that in the region from approximately 0.6 to 2 Bev the formation cross sections for the various nuclides become relatively constant as the energy of the bombarding proton increases.

In considering the results of the investigations on aluminum and copper it is useful to picture these high-energy reactions as occuring between the incoming proton and individual nucleons in the target nucleus. If the wave length of the incoming proton is long relative to nucleonic dimensions, i.e., if its energy is not very large, one would expect the nucleon-nucleon interaction cross section to vary with the energy of the incoming proton and that of the target nucleon. In addition, interactions with several nucleous are possible. As this initial collision strongly affects the subsequent cascade process, it is not surprising that excitation functions up to several hundred Mev appear different for various target and product nuclides. In this region the energy requirements of the various nuclear reactions also play a very important role in determining the nature of the excitation functions.

On the other hand, if the wavelength of the incoming proton is short relative to nucleonic dimensions, i.e., if its energy is very large, it is reasonable to expect the cross section of the initial nucleon-nucleon collision to be relatively insensitive to the proton energy. At these high energies the creation and subsequent interaction of mesons also become important. In Fig. 3 are plotted the wave lengths of nucleons and pi mesons as a function of energy.

From Fig. 3 it can be seen that the wave length of a proton becomes smaller than the dimensions of a nucleon at several hundred Mev. This is the region in which the excitation functions of the aluminum reactions become

---

[10] Miskel, Perlman, Friedlander, and Miller, Phys. Rev. 98, 1197 (1955).

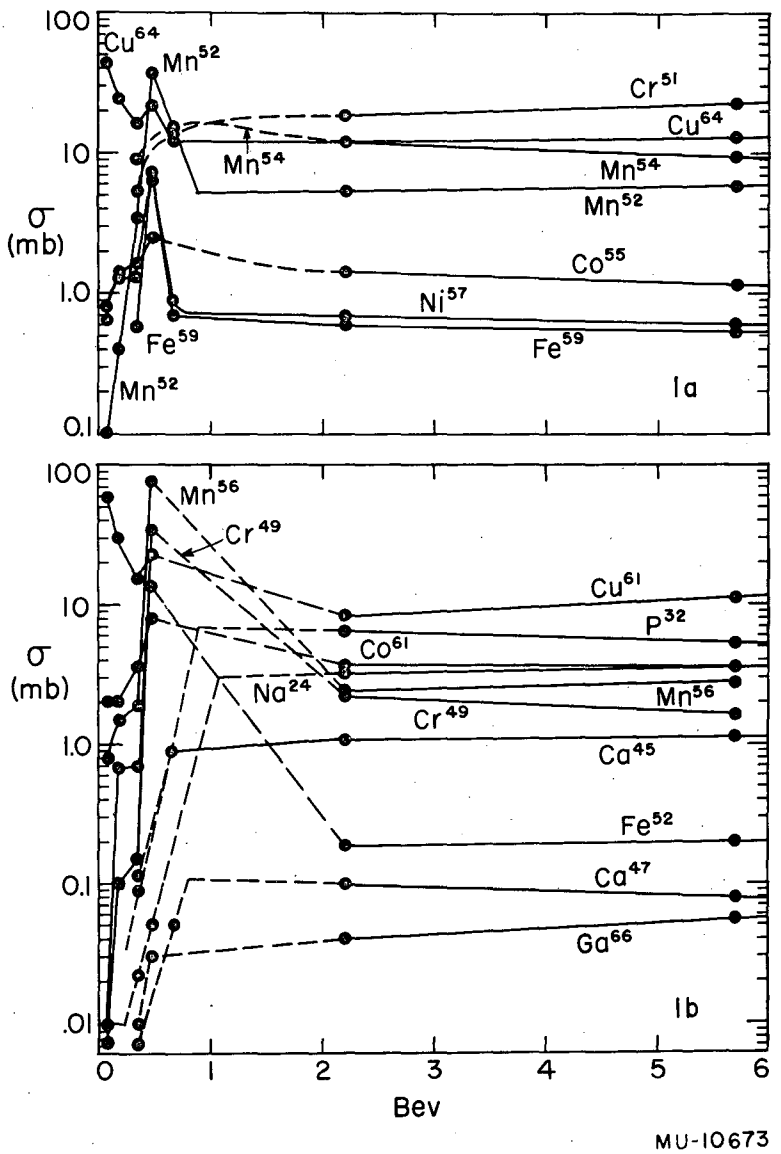

Fig. 2. Excitation functions for the production of various nuclides in the bombardment of copper by protons. Data for curves in (a) more complete than for curves in (b).

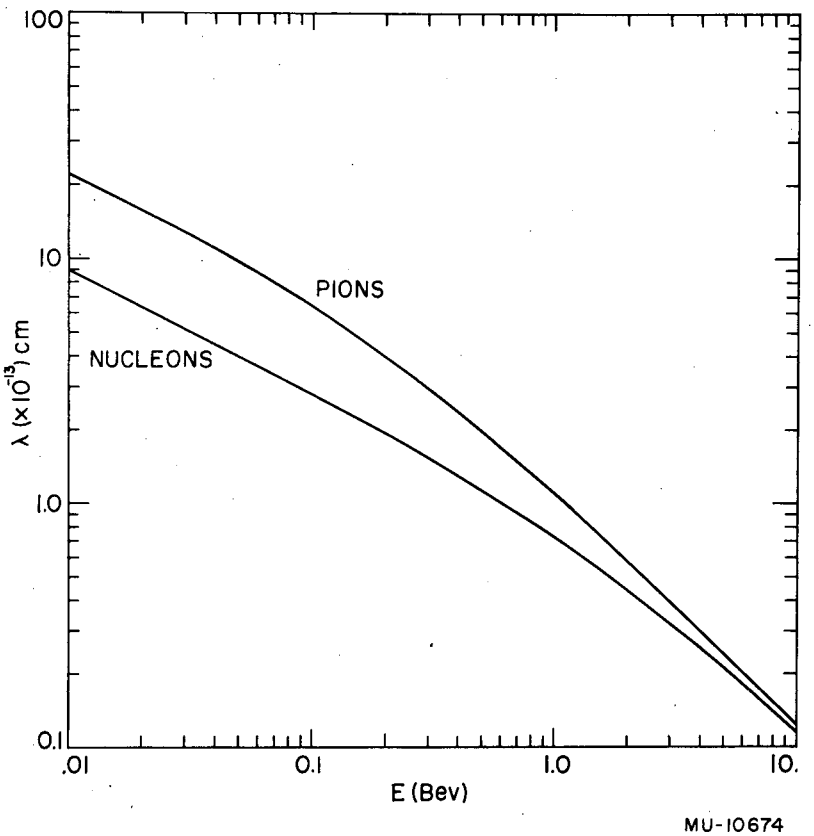

Fig. 3. Wave length of nucleons and pions as a function of energy.

flat. This is also true for copper but at a somewhat higher energy. It therefore appears that the wave length of the proton at these high energies plays an important role in the relative constancy of the cross sections.

In this energy range the formation of pi mesons becomes important. The pions thus formed have appreciably less energy than the incident proton and, according to Fig. 3 have wave lengths equal to or larger than nucleonic dimensions. We therefore expect the meson-nucleon interaction cross section to be energy-dependent. For light nuclei where the mesons have a higher escape probability this effect should be less important than for heavier nuclei.[1] Furthermore, the cascade nucleons should also have a higher escape probability in light nuclei. These two effects presumably account for the lower energy at which the excitation functions of aluminum flatten out. The peaks observed in the copper excitation functions, Fig. 2, may be due to reactions induced by mesons from the cascade process. It is difficult to see how either the initial proton or the cascade nucleons could account for these peaks. Further speculation on this point should await careful experimental work to confirm the existence of these peaks.

As the energy of the incident proton increases further, the energies of the cascade nucleons and pions also increase and hence their wave lengths decrease. The wave lengths of the pions, on the average, remain larger than those of the nucleons. In the Bev region the wave lengths of an increasingly large fraction of the cascade particles become small relative to nucleonic dimensions. Therefore, the nucleon-nucleon and meson-nucleon interaction cross sections stay relatively constant. The number of pions formed, however, continues to increase rapidly with energy. The relative constancy of the cross sections in the Bev region, despite the increased pion production, indicates that these high-energy pions may result in the emission of more nucleons, but this effect is averaged out in the formation of many residual nuclei, and hence is hardly noticeable. Careful experimental work should reveal the gradual decrease in the cross section for the formation of most nuclides with increasing energy in the Bev region.

In summary, excitation functions in the region below several hundred Mev are strongly energy-dependent as a result both of the energy requirement for various reactions and of the relatively large wave lengths of the incident and cascade nucleons. As the energy of the incident proton increases, its wave length and those of the cascade nucleons and pions decrease to less than nucleonic dimensions. The nucleon-nucleon and meson-nucleon interaction cross sections then change little as the energy of the incident proton increases. As a result and despite the increased formation of pions, the excitation functions become flat. The energy at which this occurs depends on the escape probability of the cascade pions and nucleons, and hence is larger for heavier nuclei. These considerations point to the importance of careful experimental work in the energy region above several hundred Mev and into the Bev region.

CHEMICAL ENGINEERING (PROCESS CHEMISTRY)

NOTES ON WORK IN PROGRESS

Vacuum Flow through Circular, Annular and Rectangular Sections

Walter Dong and Donald N. Hanson

Work has been continued on correlation and theoretical calculations The slip-flow equations for flow through rectangular and annular sections were derived. The effect of intermolecular collisions on the flow of gases in the molecular flow region has been studied.

Liquid-Liquid Extraction and Agitation

Theodore Vermeulen

Theoretical analysis of the extraction behavior of the system uranyl nitrate–nitric acid–water–pentaether in pulse-column runs, started by Albert F. Lane, has been continued. New material-balance relations have been derived which account for internal flow due to pulsing. The column data indicate that the aqueous-phase resistance limits uranium transfer, while the organic phase controls acid transfer.

Research to date on particle sizes in liquid-liquid agitation has been limited to uniformly sized distributions. A study of coalescence is now being initiated, with James H. Vanderveen, to determine its dependence on physical properties and its effect on drop-size distributions and mass-transfer rates.

Gas-Liquid Partition Chromatography

Robert H. Houston and Charles R. Wilke

Study of the development of engineering principles for design of equipment for gas-liquid partition chromatography continues. Chromatographic columns are being constructed for evaluation of particle size of column packing, column sizes, and lengths. Thermal conductivity cells will be used initially for an analysis of column effluent gas stream.

The Effect of Pressure on Mass Transfer in the Gas Phase

Robert J. Fallat and Charles R. Wilke

Mass transfer rates for sublimation of naphthalene pellets into air have been determined in a series of preliminary experiments covering a range of pressures. Measurements of naphthalene vapor pressures at various temperatures and pressures are in progress to aid in the interpretation of the mass transfer results.

Diffusion in Liquids

Elwood Gift and Charles R. Wilke

This work has been temporarily discontinued.

Stability of Perforated Plate Trays

Robert S. Brown, Donald N. Hanson, and Charles R. Wilke

Preliminary studies on the liquid circulating system have shown that the original manifold does not operate satisfactorily. This unit has been redesigned and will be installed shortly.

Thermal Conductivity of Gases at High Temperatures

Henry Cheung and Charles R. Wilke

A gas-mixing system consisting of two sets of storage tanks of 30-gal capacity each, a mixing tank, and associated accessories has been designed and installed.

Leak checking of the thermal conductivity cell and the gas-mixing system is completed. The equipment is ready for measuring thermal conductivity of gas mixtures.

A preliminary vacuum run with all components of the equipment operating is in progress.

Correlation of Limiting Current Density at Horizontal Electrodes under Free Convection Conditions

Eugene J. Fenech and Charles W. Tobias

Preliminary examination of the data has shown interesting trends. As was expected, the limiting current density decreased rapidly from about 40 ma/cm^2 for the 5-cm^2 electrode to approximately 20 ma/cm^2 for the 100-cm^2 and larger electrodes. A surprising result was found when the variation of limiting current density with free space above the electrode was examined. Instead of increasing with increased free space above the electrode, the limiting current density appears to actually drop as the upper boundary is moved upward. No explanation for this has been found as yet.

It has also been shown that placing vertical blocks of lucite at the extremeties of the electrodes greatly reduced the limiting current density. This result is wholly consistent with evidence found on the electrodes themselves. On the larger electrodes, 50 cm^2 and larger, three distinct regions occur; a normal central section and the two ends. Near the ends of the electrode, thin lines appear, always in the longitudinal direction of the cell, indicating the edge effects of the convection. These disappeared when end blocks were set up.

Results cited here were for approximately 0.24 M $CuSO_4$ and 1.5 M H_2SO_4.

GENERAL CHEMISTRY

METALS AND HIGH-TEMPERATURE THERMODYNAMICS

Leo Brewer, William Hicks, Geoffrey James, and Frank Greene

Molybdenum Gaseous Oxy-Halides

This work has been completed and summarized in UCRL-3144.

Ge-GeO_2 Phase Diagram

This work has been completed and summarized in UCRL-3116.

Si-SiO_2 Phase Diagram

This study has been resumed using differential thermal analysis techniques.

Thermodynamic Tables

Reports UCRL-2854 (rev.), "Heats of Sublimation of the Elements," UCRL-2992, "Free-Energy Functions of the Solid and Liquid Elements," and UCRL-3178, "Revision of the Fundamental Constants" have been completed. Further tabulations will be suspended until next summer.

Crystal Energy Calculations

This work has been summarized in UCRL-3138, "Crystal Energies for Some Transition Metal Oxides."

Composition of Carbide Vapors

Stanley G. Davis

Preparations are being made to study the composition of the vapors in equilibrium with the heated carbides of aluminum, silicon, and other metals, especially to see whether there exist gaseous molecules containing both carbon and metal. As the first step, study will be made of the atom ratio of carbon to metal in effusate from a Knudsen cell charged with the carbide, after the effusate is collected on a cold plate in high vacuum. A system for effusion and collection is being assembled. This work is part of a project using facilities financed by the Atomic Energy Commission under contract with the Institute of Engineering Research at the University.

BASIC CHEMISTRY, INCLUDING METAL CHELATES

Howard Cady, Robert Connick, Claude Coppel, James DeLap, Ladd Griffith, Robert Nickerson, Russell Sanborn, Robert Wood, Earl Worden, and Kenneth S. Pitzer

Ruthenium Chemistry

Solutions of Ru(III) prepared in this laboratory by the reduction of RuO_4 in aqueous trifluoroacetic acid appear to be complexed by the TFA. Evidence for this is the fact that Ru(III) in TFA can be eluted immediately from a Dowex 50 column with acids as low as 0.1 M. Ru(III) prepared in $HClO_4$ by $Sn(ClO_4)_3$ reduction is different, and takes about 48 cc of 0.34 M $Mg(ClO_4)_2$ to reach the bottom of the column. Cu(II) is eluting in 8 cc and Fe(III) in 17 cc under the same conditions.

The Ru(III) in $HClO_4$ had very low absorption.

Wave length (mμ)	ε
800 mμ to 450 mμ	2.5
425	13
400	30
380	35 (peak)
375	34
350	26
325	25
300	26
275	125
250	1000
225	2200 (peak)
2125	1900

The solution is 0.34 M in Mg_2ClO_4,

0.68 M in $HClO_4$,

1.80×10^{-4} M in Ru(III).

This solution shows no signs of oxidation after a period of 1 month at room temperature and exposure to air. The stock solution containing an excess of Sn^{++} initially has been oxidized and is evolving RuO_4 slowly.

Kinetics of Rapid Reactions

The calculations of mixing time and bubble formation, which were reported earlier, have been completed. The mixing-time calculation was extended to a three-dimensional diffusion problem, which, however, did not affect earlier conclusions. This calculation indicates that our present moving-baffle type mixers will be limited to mixing times of the order of 10^{-2} to 10^{-3} second. To go beyond these limits would require tremendous forces (approximately 20,000 lb). The same time range also seems to be the time limit in which the desired amount of reactants can flow through any practical turbulator plate. At 10^{-3} second, calculations indicate 90% of turbulator plate must be orifice area.

The bubble-formation calculations were inconclusive. When calculation was made by two methods--straight diffusion considerations, and with accomodation coefficients--similar results were obtained. These results, however, predicted that there should be no bubble formation under conditions where bubbles are known to form. This calculation will be checked.

Since mixing times of the order of 10^{-2} to 10^{-3} second still give us a very useful range in which to work, the present work is in preparing a new mixer and a new baffle for the old mixer, which will eliminate the premixing problem.

The new mixer has been completed and is at present being studied, with the hope of using it shortly to study some reaction rates. It is a 1-cm single-baffle plexiglass mixer with beveled edges to give tight seals on all sides. It gives no premixing and with the present firing mechanism, fires in approximately 10^{-2} second or less.

Polarographic Studies

The work in this field this quarter has primarily consisted of cleaning, assembling, and becoming familiar with the equipment. Considerable library work has been done. Plans are indefinite at this time as to the systems to be studied.

Radiation-Induced Reactions in Nonaqueous Solutions

The study of the photolysis of α-α-diphenyl-β-picryl-hydrazyl(DPPH) in chloroform solutions is being continued. The source used in the photolysis of DPPH in chloroform is a Hanovia medium-pressure mercury arc, Type 16,200. Light of wave length 2537 A and 2650 A is isolated by the use of two centimeters of saturated nickel sulfate solution, 1 centimeter of Cation-X (0.2 g per liter), and a Corning 9863 filter of 2 mm thickness. The intensity of the radiation reaching the reaction cell is about 1.4×10^{16} quanta per second per liter.

The disappearance of DPPH is measured calorimetrically by the disappearance of the 5300 A absorption band in the visible spectrum of DPPH with a Beckman quartz spectrophotometer, Model DU. The disappearance of the DPPH is linear with time within experimental error for the first 10% of disappearance. The rate of disappearance is independent of dissolved air.

An attempt is being made to measure the quantum yield of the disappearance of DPPH under the conditions mentioned above. In a concentration range of 1.0×10^{-5} to 1.0×10^{-4} mole DPPH per liter of $CHCl_3$ solution, the quantum yield appears to have the constant value of $0.12 \pm .02$. The stability of the DPPH solutions in $CHCl_3$ and the rate of photolysis of DPPH are critically dependent upon the degree of purity of the chloroform. It is very difficult to get reproducible results from different samples of chloroform that has been distilled in air. Experiments are now being done with solutions prepared entirely in vacuum in an attempt to confirm the constancy of the quantum yield at these concentrations. An attempt is also being made to determine the efficiency of DPPH as a free-radical scavenger of small organic free radicals, by applying the results of the photochemical studies.

Determination of the Molecular Structure of Aluminum Hydride

By means of the techniques of high- and low-resolution nuclear magnetic resonance, an attempt will be made to determine the molecular structure of aluminum hydride and thus the type of bonding involved. This work will consist of two phases. The first will be the use of high-resolution nuclear magnetic resonance to study the reactions forming the hydride in solution and its behavior after formation, and thus obtain a clue as to the method of formation. The second phase will involve studying the solid, measuring absorption line widths at various temperatures, and making theoretical calculations based on possible molecular structures. The answers are to be compared with the experimental results.

A study of the Mechanism of Electroreduction at the Dropping Mercury Electrode

This work has been completed and is being published in UCRL-3213.

Heat of Formation of the Ferrate Ion

The heat of the reaction of aqueous potassium ferrate with 1 N perchloric acid to form aqueous ferric perchloric, oxygen, and water is being measured. From this the heat of formation of potassium ferrate will be calculated.

Acetaldehyde, t

An apparatus has been constructed for obtaining samples of tritiated acetaldehyde and the products of its pyrolysis for counting in a scintillation counter. A sample of the tritiated acetaldehyde prepared for use was placed in the counter. Indications are that the tritiated acetaldehyde has a specific concentration of tritium too high for counting with the equipment to be used. Provisions are now being made to dilute the tritiated acetaldehyde with normal acetaldehyde in order to obtain a source of tritiated acetaldehyde of the proper concentration of tritium for counting. This acetaldehyde will be pyrolized and the isotope effect will be determined.